TKK Dissertations 211
Espoo 2010

FINITE-ELEMENT ANALYSIS OF EDDY CURRENTS IN THE FORM-WOUND MULTI-CONDUCTOR WINDINGS OF ELECTRICAL MACHINES

Doctoral Dissertation

Mohammad Jahirul Islam

Helsinki University of Technology
Faculty of Electronics, Communications and Automation
Department of Electrical Engineering

TKK Dissertations 211
Espoo 2010

FINITE-ELEMENT ANALYSIS OF EDDY CURRENTS IN THE FORM-WOUND MULTI-CONDUCTOR WINDINGS OF ELECTRICAL MACHINES

Doctoral Dissertation

Mohammad Jahirul Islam

Dissertation for the degree of Doctor of Science in Technology to be presented with due permission of the Faculty of Electronics, Communications and Automation for public examination and debate in Auditorium S4 at Helsinki University of Technology (Espoo, Finland) on the 4th of January, 2010, at 12 noon.

Helsinki University of Technology
Faculty of Electronics, Communications and Automation
Department of Electrical Engineering

Teknillinen korkeakoulu
Elektroniikan, tietoliikenteen ja automaation tiedekunta
Sähkötekniikan laitos

Distribution:
Helsinki University of Technology
Faculty of Electronics, Communications and Automation
Department of Electrical Engineering
P.O. Box 3000
FI - 02015 TKK
FINLAND
URL: http://sahkotekniikka.tkk.fi/
Tel. +358-9-470 22384
Fax +358-9-470 22991
E-mail: jahirul.islam@se.abb.com

ISBN 978-952-248-254-9
ISBN 978-952-248-255-6 (PDF)
ISSN 1795-2239
ISSN 1795-4584 (PDF)
URL: http://lib.tkk.fi/Diss/2010/isbn9789522482556/

TKK-DISS-2721

Picaset Oy
Helsinki 2010

ABSTRACT OF DOCTORAL DISSERTATION	HELSINKI UNIVERSITY OF TECHNOLOGY P.O. BOX 1000, FI-02015 TKK http://www.tkk.fi

Author Mohammad Jahirul Islam

Name of the dissertation
Finite-element analysis of eddy currents in the form-wound multi-conductor windings of electrical machines

Manuscript submitted 23.02.2009	Manuscript revised 05.06.2009
Date of the defence 04.01.2010	
☐ Monograph	☒ Article dissertation (summary + original articles)

Faculty Electronics, Communications, and Automation
Department Electrical Engineering
Field of research Modelling of electrical machines
Opponent Professor Oszkár Bíró
Supervisor Professor Antero Arkkio
Instructor

Abstract

The aim of this research was to develop comprehensive numerical models for considering eddy currents and circulating currents in the form-wound multi-conductor windings of electrical machines and to study the effects of eddy currents and circulating currents. Time-harmonic and time-discretised finite-element methods were developed. The methods were applied to the stator winding of a 1250-kW cage induction motor and in both the stator and rotor windings of a 1.7-MW doubly-fed induction generator (DFIG). The series and parallel connections of the winding were taken into account. The Newton-Raphson iteration method was used to solve the system of non-linear equations. In time-harmonic FEM, the system of equations was solved iteratively just once for the steady-state solution. In time-discretised FEM, the system of equations was solved iteratively at every time step. The backward Euler method was used for the time discretisation.

The radial distance of the stator bars from the air gap has a remarkable effect on losses and was found to be an important design parameter. A significant amount of stator-winding eddy-current loss can be reduced by considering this design parameter. A transposition of the conductors was implemented to reduce the circulating currents between the parallel stator conductors. The eddy-current effects in the form-wound multi-conductor windings of electrical machines were studied for both a sinusoidal and non-sinusoidal supply. A pulse-width-modulated (PWM) voltage supply was achieved by sinus triangle comparison and used as a non-sinusoidal supply for the machine. A PWM supply produced a significant amount of additional eddy-current losses in the form-wound stator winding of the cage induction motor when compared to the sinusoidal supply. The fundamental harmonic voltages of the sinusoidal and PWM supplies were equal for comparing the results. Similar sinusoidal and PWM voltages were used to supply the rotor winding of the DFIG as well. The additional eddy-current losses in the form-wound rotor winding as a result of the PWM supply were small.

Keywords eddy currents, finite-element analysis, form-wound, multi-conductor winding, cage induction motor, doubly-fed induction generator

ISBN (printed) 978-952-248-254-9	ISSN (printed) 1795-2239
ISBN (pdf) 978-952-248-255-6	ISSN (pdf) 1795-4584
Language English	Number of pages 144

Publisher Department of Electrical Engineering, Helsinki University of Technology

Print distribution Department of Electrical Engineering, Helsinki University of Technology

☒ The dissertation can be read at http://lib.tkk.fi/Diss/2010/isbn9789522482556

Preface

This research was conducted in the Electromechanics team at the Department of Electrical Engineering of Helsinki University of Technology. This work was financed by ABB Oy and Helsinki University of Technology.

I would like to express my sincere gratitude to my supervisor, Professor Antero Arkkio, for his constructive supervision, devoted expertise, encouragement, intensive discussion, critical comments, and proper direction and support. The support and encouragement of the former head of the Laboratory of Electromechanics, Prof. Asko Niemenmaa, are highly appreciated. I would like to thank Emeritus Professor Tapani Jokinen, Dr. Jarmo Perho, Dr. Anouar Belahcen, Dr. Anna-Kaisa Repo, and Dr. Emad Dlala for their constructive comments and discussion. I remain grateful to Jenni Pippuri for her various kinds of discussion and help. I am thankful to Mr. Ari Haavisto and Mrs. Marika Schröder for their assistance and help. I thank all of my colleagues for their friendly behaviour and for creating a pleasant environment to work in.

I am thankful to Mr. Jukka Järvinen, Dr. Áron Szücs, and Mr. Jari Pekola, ABB Oy, for their technical support and the fruitful discussions we had about various practical matters.

I would like to express my heartfelt gratitude to my parents, who greatly motivated me to take up the challenge. My dearly beloved brothers, sisters, nephews, and nieces are gratefully acknowledged for their continuous support, kindness, encouragement, and care.

Finally, I would like to deeply thank my beloved wife, Israt, and daughter, Kashfiya, for their love, smiles, sacrifice, patience, and continuous support to me in passing through this tough time.

Mohammad Jahirul Islam

List of publications

P1 Islam, M. J.; Pippuri, J.; Perho, J.; Arkkio, A. 2007: “Time-harmonic finite-element analysis of eddy currents in the form-wound stator winding of a cage induction motor”, *IET Electric Power Applications*, Volume 1, Issue 5, September 2007, pp. 839–846.

P2 Islam, M. J.; Arkkio, A. 2008: “Time-stepping finite-element analysis of eddy currents in the form-wound stator winding of a cage induction motor supplied from a sinusoidal voltage source”, *IET Electric Power Applications*, Volume 2, Issue 4, July 2008, pp. 256–265.

P3 Islam, M.J.; Arkkio, A. 2009: “Effects of pulse-width-modulated supply voltage on eddy currents in the form-wound stator winding of a cage induction motor”, *IET Electric Power Applications*, Volume 3, Issue 1, January 2009, pp. 50–58.

P4 Islam, M. J.; Arkkio, A. 2008: “Optimum supply for an inverter-fed cage induction motor at different load conditions”, Proceedings of *Nordic Workshop on Power and Industrial Electronics*, 9 – 11 June 2008, HUT, Finland, 7 p. Available: http://lib.tkk.fi/Conf/2008/urn011711.pdf

P5 Islam, M. J.; Arkkio, A. 2008: “Finite-element discretisation for analysing eddy currents in the form-wound stator winding of a cage induction motor”, *CD proceedings of the 14th International Symposium on Electromagnetic Fields in Mechatronics, Electrical and Electronic Engineering*, 10 – 12 September 2009 Arras, France, 6 p.

P6 Islam, M. J.; Arkkio, A. 2009: “Finite-element analysis of eddy currents in the form-wound multi-conductor windings of a doubly-fed induction generator”, *Report Series on Electromechanics,* Report 75, Helsinki University of Technology, Espoo 2009, 20 p. ISSN 1456-6001, ISBN 978-952-248-206-8.

Contents

List of symbols and abbreviations

$\boldsymbol{A}$	magnetic vector potential
a	nodal value of the magnetic vector potential
$\boldsymbol{B}$	magnetic flux density
$\boldsymbol{E}$	electric field strength
$\boldsymbol{H}$	magnetic field strength
h_{sb}	distance from the inner surface of the stator to the top of the stator bars
$\boldsymbol{J}$	current density
i_m	current of the m^{th} phase
k_{eddy}	eddy factor
l_{e}	effective length of the machine
L_{e}	end winding inductance of a phase
$P_{\mathrm{ew}}^{\mathrm{s}}$	resistive loss of stator end winding
$P_{\mathrm{sb}}^{\mathrm{s}}$	resistive loss in the slot-embedded part of stator winding
$P_{\mathrm{t}}^{\mathrm{s}}$	total resistive loss of stator winding
Q_{b}	number of bars of the winding in the solution region
Q_{ss}	number of symmetry sectors
Q_m	number of stator phases
R	DC resistance of a phase
R_{b}	DC resistance of a bar
R_{e}	end-winding DC resistance of a phase
R^{str}	DC resistance of a strand
S_n	cross-section area of the n^{th} bar of the winding
t	time
u_n^{b}	potential difference of the n^{th} bar
u_m	voltage of the m^{th} phase
σ	conductivity
ν	reluctivity

μ permeability

ϕ electric scalar potential

ω angular frequency of time variation

Ω solution region

Abbreviations

2-D two-dimensional

3-D three-dimensional

AC alternating current

CIM cage induction motor

DC direct current

DFIG doubly-fed induction generator

FEA finite-element analysis

FED finite-element discretisation

FEM finite-element method

HBM harmonic-balance method

PWM pulse-width modulation

rms root mean square (effective value)

THA time-harmonic analysis

TSA time-stepping analysis

1 Introduction

1.1 Background

The efficient, reliable, and economical design of electrical machines has been a standard demand for researchers and engineers since the very beginning of electrical engineering. As a result, electrical machines have good efficiency. For example, in Finland approximately 65% of electrical energy is consumed by electrical motors and practically all electricity is produced by rotating electrical machines. Even a small improvement in efficiency can give a significant amount of financial savings. To design even more efficient machines requires accurate knowledge of the magnetic field distribution and consideration of the detailed electromagnetic phenomena. One of these phenomena is eddy currents in the windings of electrical machines. It is an interesting field of engineering to design even more efficient and reliable electrical machines.

The development of solution methods and high-speed computers has made it possible to solve ever more complicated electromagnetic field problems. The finite-element method has proved an efficient tool when dealing with complicated geometries such as electrical machines (Chari & Silvester 1971). Two-dimensional (2-D) approximation has proved to be a powerful tool in the analysis of radial-flux electrical machines. With sinusoidal approximation (time-harmonic analysis), the problem can be greatly simplified and the model can be very time-efficient. However, it cannot consider properly the rotation, and magnetic saturation of the machine. A time-discretised finite-element analysis is required to model these phenomena more accurately.

The speed control of electrical motors is needed in many applications in industry. As a consequence, frequency converters to supply electrical machines are becoming more popular (Boglietti et al. 1996). When a motor is supplied from an inverter, the control of the motor becomes easier and more accurate, but this makes the supply voltage non-sinusoidal, which means that it contains a set of harmonics (Fouladgar & Chauveau 2005). These additional voltage harmonics inject flux harmonics into the motor and produce current harmonics. Speed control produces significant energy savings in many pump, fan, and compressor applications, but in electrical machines, the amount of power loss increases significantly (Arkkio 1991, Hilderband & Roehrdanz 2001, Lee et al. 2004, Oberretl 2007).

In the multi-conductor windings of electrical machinery and devices, the proper estimation of eddy currents is needed for successful design. It is very important to model the eddy currents in the form-wound multi-conductor winding accurately and analyse and optimise them at the design stage in order to have an efficient and reliable machine. The machine designers can move in the wrong direction if they neglect or underestimate the effects of eddy currents by considering them with simplified analytical calculations.

1.2 Objectives

The main objective of the thesis is to develop accurate numerical models for considering eddy currents and circulating currents in the form-wound multi-conductor windings of electrical machines. The results of models with sinusoidal and non-sinusoidal supplies are analysed in order to estimate the contribution of eddy-current effects to power losses. The local hot spots are predicted from the loss analysis. Two types of induction machines are considered in order to study the eddy-current effects in form-wound multi-conductor stator and rotor windings.

1.3 Scientific contribution

- Combined finite-element circuit model is developed for time-harmonic analysis of eddy currents in form-wound multi-conductor windings. This model can also be used to study circulating currents between parallel conductors. It is applied to the stator winding of a 1250-kW cage induction motor and to both the stator and rotor windings of a 1.7-MW doubly-fed induction generator. The time-harmonic finite-element method (FEM) is mainly used to compute initial values for time-discretised FEM, but, because of its time efficiency, it can also be used to study the eddy currents and circulating currents caused by the fundamental harmonic.

- Time-discretized finite-element circuit model is developed to analyse the eddy currents and circulating currents in form-wound multi-conductor windings. The method is applied to the same machines as the time-harmonic approximation above. The finite-element model that is developed is used to study the effects of eddy currents caused by the higher harmonics from the stator and rotor slottings and the rotation of the rotor. The high-frequency components mainly cause eddy-current losses in the conductor near to the air gap.

- Time-discretised FEM is used to study the effects of eddy currents in form-wound stator windings resulting from the non-sinusoidal supply. A pulse-width-modulated (PWM) voltage source is used to supply the stator of a 1250-kW cage induction motor. The significance of the modelling of eddy currents in the stator winding is further weighted because of the inverter supply.

- Time-discretised FEM is used to study the effects of eddy currents as a result of the frequency-converter supply in the form-wound rotor winding of a 1.7-MW doubly-fed induction generator. Because of the higher value of the self-inductance of the rotor winding with respect to stator inductance, the additional eddy-current loss in the rotor caused by the PWM supply remains small.

- The radial distance from the inner surface of the stator to the first bar in a stator slot has remarkable effects on the losses and it is found to be an important design parameter in minimising the losses in the stator winding. According to the results, the eddy-current loss in a bar can be dangerously large and has to be modelled properly in the design of a machine.

- The circulating currents in the parallel stator conductors are modelled and implemented in order to study the effect of the transposition of the form-wound winding. A systematic transposition reduces the circulating currents to a negligible level.

1.4 Structure of the dissertation

The thesis is organised in the following way:

- Chapter 1 includes the background, motivation, and aim of the work. The scientific contributions and a short summary of the publications are presented.
- Chapter 2 presents a literature study of eddy currents in multi-conductor winding.
- Chapter 3 presents the methods of analysis. It consists of an overview of the electromagnetic field, the basic equations, and the finite-element analysis of eddy currents in the stator and rotor winding of electrical machines.
- Chapter 4 presents the simulations and numerical results of the eddy currents of form-wound stator windings for the 1250-kW cage induction motor and of the stator and rotor windings of the 1.7-MW doubly-fed induction generator (DFIG).

This chapter also contains a verification of the eddy-current model and power balance to justify the methods.

- The results are discussed and summarised in Chapters 5 and 6.

The publications that are included are reprinted at the end of the dissertation.

1.5 Publications

Publication P1

The basic mathematical formulations are presented in publication P1. The basic equations are derived in matrix form to be implemented in the time-harmonic finite-element model. The calculation of eddy-current and circulating-current losses in the multi-conductor stator winding of a cage induction motor is presented. In the model, the eddy-current formulation of the series and parallel connected stator bars is solved, together with the circuit and field equations, using a 2-D time-harmonic approximation. The eddy-current loss distribution of the stator bars and the quantitative results of eddy-current and circulating-current losses were studied with two different conductor arrangements inside the stator slots. The radial position of the stator bars was pointed out as a design parameter to build up a more efficient and reliable machine. The eddy-current model was verified with an analytical method.

The paper was developed and written by Islam. Professor Arkkio contributed by means of comments, suggestions, and his expertise in the field of finite-element analysis. Pippuri and Arkkio implemented the analytical method for verification. Pippuri contributed by writing the verification part and making the study of German literature. Perho contributed with valuable comments and discussion.

Publication P2

A time-discretised finite-element method is developed to study the eddy-current effects of multi-conductor form-wound stator winding resulting from the fundamental and high-frequency magnetic flux in a cage induction motor. The Backward Euler method is used to discretise the time dependence of the electromagnetic field, circuit variables, and the motion of the rotor. The motor is supplied from a sinusoidal voltage source. To study the eddy-current losses produced by the high-frequency flux resulting from the stator and rotor slots and motion of the rotor, the results are compared with the results from the time-harmonic model. The model was verified with an analytical method.

The paper was developed and written by Islam. Professor Arkkio contributed by means of comments, suggestions, and his expertise in the field of finite-element analysis.

Publication P3

Publication P3 presents the eddy-current effects of a form-wound multi-conductor stator winding of a 1250-kW cage induction motor resulting from a non-sinusoidal supply voltage. The time-discretised finite-element model developed in publication P2 is used. A pulse-width-modulated (PWM) voltage is used to supply the motor. To study the eddy-current losses caused by the high-frequency flux generated from the PWM supply, the results are compared with the results obtained from a sinusoidal voltage supply.

The paper was developed and written by Islam. Professor Arkkio contributed by means of comments, suggestions, and his expertise in the field of finite-element analysis.

Publication P4

Publication P4 searches for an energy-efficient power supply for an inverter-fed cage induction motor under different light-load conditions. The fundamental harmonic terminal voltage is reduced from its rated value and the value of the slip is adjusted to achieve a particular load condition. Loads of 25%, 50%, and 75% of the rated load are studied. If the load is less than 50%, a significant amount of loss can be reduced if there is a possibility of adjusting the DC-link voltage.

The paper was developed and written by Islam. Professor Arkkio contributed by means of comments, suggestions, and his expertise in the field of finite-element analysis.

Publication P5

Publication P5 studies the finite-element discretisation (FED) needed for the proper analysis of eddy currents in the form-wound stator winding of a 1250-kW cage induction motor. To study the accuracy of the FED, the number of finite elements per bar is increased by making a more detailed subdivision over the bar height and width. Two main supply conditions for a cage induction motor, sinusoidal and PWM are considered.

The paper was developed and written by Islam. Professor Arkkio contributed by means of comments, suggestions, and his expertise in the field of finite-element analysis.

Publication P6

Publication P6 studies the eddy currents in the form-wound stator and rotor winding of a doubly-fed induction generator. The time and space dependence of the field and circuit variables and the motion of the rotor are modelled with time-discretised finite-element analysis. The stator is supplied from a sinusoidal voltage source, as it is connected to the grid. The rotor is supplied with a PWM supply from a constant DC-link voltage. To compare the effects of eddy currents resulting from the frequency-converter supply, a sinusoidal voltage source in the rotor supply is also considered. The additional eddy-current loss caused by the PWM supply is small compared to the loss resulting from a sinusoidal supply.

The paper was developed and written by Islam. Professor Arkkio contributed by means of comments, suggestions, and his expertise in the field of finite-element analysis.

2 Literature study

The time variation of the magnetic field induces eddy currents causing a non-uniform distribution of current density on the cross-section of a conductive body. This results in an increase in the resistive loss as compared with the DC resistive loss (Lammeraner and Štafl 1966). The eddy currents are one of the main problems encountered in designing electrical equipment such as electrical machines, transformers, or inductors. Consequently, their determination has been an interesting topic for researchers and engineers since the very beginning of electrical engineering. The eddy-current problem is more often recognised as a skin-effect problem, but if there are several current-carrying conductors then the problem is a combination of skin and proximity effects. In a multi-conductor system, the skin effect is defined as the phenomenon in which the current density in a current-flowing conductor is crowded towards the surface because of its own time-varying magnetic field. When the current density of a conductor is influenced by the magnetic field of a neighboring current-carrying conductor, the phenomenon is called the proximity effect. Both the skin and proximity effects cause a non-uniform current distribution called the eddy-current effect. A general overview on the existing literature of published articles and books of the eddy-current problems is presented in this chapter. The overview is presented in chronological order.

The "depth of penetration" or "skin depth" (Lammeraner & Štafl 1966, Stoll 1974) is probably the most commonly used analytical term that defines geometrical parameters used to understand the eddy-current effects. For a sinusoidally varying magnetic field, in a conducting material of a semi-infinite plate with a surface on the *x*-*y* plane, the variation of the current density in the *z*-direction can be presented as (Bastos & Sadowski 2003)

$$J(z,t) = J_0 \mathrm{e}^{-z/\delta} \cos(\omega t - z/\delta) \qquad (1)$$

where J_0 is the surface current density, ω is the frequency, and δ is the skin depth defined as

$$\delta = \sqrt{\frac{2}{\omega \sigma \mu_0 \mu_\mathrm{r}}} \qquad (2)$$

where σ is the conductivity, μ_0 is the magnetic permeability of free space, and μ_r is the relative permeability of the conducting material. The equations are based on the assumption of a quasi-steady state, with a constant frequency, and with the electric and magnetic conductivities of the materials under consideration remaining constant. At a 50-Hz supply frequency, the depth of penetration is about 9.4 mm for a copper conductor.

The first analytical formulation of eddy currents in slot-wound conductors was introduced by Field (1905) at the beginning of the 20^{th} century. A qualitative description of the effects of eddy currents was presented. The types of conductors were limited to solid and infinitely stranded or laminated ones and the winding arrangement was such that there were no conductors of different phases in the same slot. The author studied the effect of eddy currents resulting only from the leakage flux that passes circumferentially from one stator tooth to another through the conductors. The effect of the main flux that passes from the air gap to the stator slot radially was omitted from the study.

Gilman (1920) presented analytical calculations of the eddy currents for a finite number of stranded conductors that are embedded in a slot, as well as the phase relation of the strands. The author also pointed out the fact that the main flux that enters the top of the slot adjacent to the air gap causes the eddy-current loss. He suggested that this loss can be regulated by using overhanging tooth tips, sunken coils, or magnetic wedges. However, the eddy-current loss resulting from the main flux was not considered in that study. Dwight (1945) presented a power series in frequency by developing the ratio of effective resistance to DC resistance in a flat conductor of finite width.

Richter (1951) studied the effect of eddy currents for a given main flux with analytical formulations for different kinds of simple models. Another important study can be found in Oberretl (1969), where the author gives thirteen rules to minimise the losses of electrical machines. Rule number seven mainly prescribes the position of the stator coil and rotor bar. The conclusive rule is based upon the analysis of the so-called analogue network method (Oberretl 1963, Oberretl 1969). The method solves the partial-differential equation by making an analogue network with semiconductor diodes, a capacitor, and resistors (Oberretl 1969). For an open stator slot, the ratio between the width of the stator slot and the height from the inner surface of the stator to the top of the stator bar must be less than or equal to three. However, the rule seems to be defined for too wide a range.

Lammeraner & Štafl (1966) and Vogt (1972) mainly summarised the basic principles of analytical eddy-current loss calculation for the solid and stranded conductors of electrical machines. They calculated the eddy-current losses of the coil analytically, as well as defining the *effective resistance* and *resistance coefficient* (the ratio between the effective resistance and the DC resistance). An overview of the analytical formulations of eddy currents is presented by Stoll (1974) for one- and two-dimensional problems.

However, the analytical method is mostly restricted to studying the effect of the circumferential flux. There are some analytical formulations for a given radial main flux (Richter 1951). In addition to the leakage flux, the time-varying main flux that penetrates into the slot from the air gap produces an additional eddy-current loss (Gilman 1920, Demerdash et al. 1975). However, an exact analytical model is unfortunately not possible because of the complicated geometry of the slot region and nonlinearities of the magnetic iron core (Dabrowski & Demenko 1988).

With the development of computers, the invention and usability of different kind of numerical methods have increased. There are different kinds of numerical formulations or approaches to handling multi-conductor eddy-current problems. To reduce the memory requirement or computational time, the numerical achievements from the early years of electromagnetic FEM are still useful. The trade off between the accuracy and computational time is always a concern even with the availability of the fast computers and software packages.

Silvester proposed the modal network theory to consider skin effect in a flat conductor (1966). Instead of solving a differential or integral equation directly, the author attempted to find the normal modes of the current distribution from the Eigen-value problem and then solve the skin-effect problem by using an equivalent network. The theory was applied to calculate the AC resistance and reactance of an isolated conductor (Silvester 1967). The author applied the theory to a complicated conductor shape (Silvester 1968). By using this theory he also predicted the skin effect of multi-conductor and multi-phase systems (Silvester 1969, Silvester et al. 1972).

Demerdash & Hamilton (1972a) modelled the magnetic field of a four-pole 699 MVA and of a two-pole 733 MVA turbo-generator. They used finite-difference techniques based on magnetic vector potential formulation (Demerdash et al. 1972) to study the eddy-current loss resulting from the main flux and rotor asymmetry (Demerdash & Hamilton 1972b). Long & Hamilton (1975) presented a simplified technique to calculate the eddy-current loss induced in stator conductors by the radial flux of cylindrical rotor synchronous generators. The losses in the stator conductors were calculated from the solution of the air-gap flux-density waveform. The technique combined the vector potential with the grid modelling method. They eliminated the stator conductors from the slots during the load conditions and neglected the effect of leakage flux in order to simplify the problem. This means that the influence of the eddy currents on the magnetic field distribution in the slot was neglected. Carpenter (1975) used a coupled network approach and McWhirter et al. (1979) used Fredholm integral equations to handle the eddy-current problem.

Finite-element analysis is widely used and is probably the most efficient tool to model eddy currents in multi-conductor windings. Chari & Csendes (1977) presented a 2-D finite-element analysis of the skin effect in a current-carrying conductor. The authors made a comparison of the results with the traditional one-dimensional analysis. Demerdash & Nehl (1979) made a comparative evaluation between the finite-element and finite-difference techniques. The article covered the aspects of effectiveness, numerical accuracy, and implementation, as well as computer storage and execution time. For solving a non-linear electromagnetic field problem, the finite-element method was a better option compared to the finite-difference method.

The superposition approach was used by Preis et al. (1982) and Preis (1983) to calculate the eddy-current loss in a multi-conductor system. The superposition method assumes that it is possible to find a finite-element solution of the field if the current density in the field equation is given. For N conductors, the problem can be solved by solving the field equation N times. Each time, a different conductor is assumed to carry a unit current density instead of the source current, while the net current in all the other conductors is assumed to be zero. The final solution is obtained in a straightforward manner from the principle of superposition. However, the approach is useful only if the system is totally linear.

Konrad (1981, 1982) presented what is probably the most popular method based on integrodifferential approach. In this approach, both the vector potential and the source current are treated as unknown. The total current density is the summation of the source current density and the induced current terms. By making a surface integral over the cross-section of the conductor, the source current density term can be presented as a function of the total current and an integral term and replaced in the field equation. The field equation can then be solved for a given total current of the conductor. Since there are a differential term and an integral term in the field equation, the approach was named an integrodifferential approach. To make a comparative study between the superposition and integrodifferential approaches, Konrad et al. (1982) implemented the same problem with both the approaches. The authors found an added advantage of the integrodifferential formulation in that it was a direct method requiring neither iteration nor Eigen functions to solve the linear steady-state skin-effect problem in multi-conductor systems.

Weiss & Csendes (1982b) presented another approach by adding an extra equation for each conductor for multi-conductor busbars. The source current in the field equation was kept unknown and two unknowns (source current-density vector and magnetic vector potential) were solved from differential and algebraic equations. This means that they built up a coupled system to solve a classical steady-state skin-effect problem. The same method was applied to solve the skin-effect problem for an inverse "T-slot" problem (Weiss & Csendes 1982a). In this article, they generalised the formulation to include both the multi-conductor busbars and slot-embedded conductor. The formulation to calculate the eddy-current loss from the current density in a multi-conductor system was presented by Weiss et al. (1983). This coupled-system approach was used to solve different kinds of applications of multi-conductor eddy-current problems. For example, the approach was used by Weiss & Garg (1985) for axi-symmetric geometry with rotational symmetry. In multiple excited magnetic systems, the transient (Garg & Weiss (1986), Weiss & Garg (1989)), and steady-state (Weiss & Garg 1988) electromagnetic field problems were solved for arbitrary terminal voltages. The steady-state solution was obtained with time-harmonic approximation and time-discretised FEM was used to solve the transient problems.

Dabrowski & Demenko (1988) presented a hybrid method to analyse the eddy-current loss in the rectangular bars in the stator slot of an electrical machine as a result of the main flux. The technique was called a hybrid one because of its connection of numerical and analytical calculations. An analytical formulation was developed that was based on the damping coefficient that was obtained from reluctance-network based numerical calculations. In their study, they neglected the isolating gap between the bars and used the constant amplitude of flux for a slot pitch.

Tsukerman et al. (1992) proposed a general formulation to deal with time-dependent eddy-current diffusion problems. The electromagnetic field was computed in 2-D and the circuit equation with terminal voltage for each conductor was taken into account. The global system of equations was constructed by adding an extra integral equation to link the field and circuit equations where the loop currents were expressed in terms of total current. The approach is based on the integrodifferential finite-element formulation with the conventional loop-current method of circuit theory. As a numerical example of the proposed formulation, they considered three rectangular busbars with eddy currents and external circuit connection.

The harmonic losses in the stranded conductor generally found in AC machines were investigated by Salon at al. (1993) using finite-element analysis (FEA) with circuit constraint. An analytical formula was developed and compared with the finite-element analysis for a given flux density, frequency, and conductivity. The analytical formula ignores the effect of eddy currents on the field. At lower frequencies, the agreement between the FEA and the closed-form analytical formula was good, but at high frequencies, the results did not agree well.

An overview of the numerical formulations of 2-D eddy-current problems was presented by Tsukerman et al. (1993a). The authors explained a way of handling eddy-current problems with and without the circuit equation. The article presented a procedure for how to solve the filamentary problem in which conductors are composed of thin filaments and the current distribution is predetermined. In this case, the current density is not a function of the vector potential. They also presented the eddy-current problems for solid conductors where the current density is unknown because it is related to the magnetic vector potential. A survey of the transient eddy-current problems was presented by Tsukerman et al. (1993b) with different kinds of finite-element formulations. The article went through the time-discretised finite-element analysis and short descriptions of different types of system solvers and their efficiency, and, finally, included some numerical examples.

Krawczyk & Tegopoulos (1993) published a book that gives a very good summary of the numerical modelling of eddy currents. The book starts with a survey of the previous work and continues with quantities to describe the eddy-current problems, for example, field variables and potentials. Different kinds of mathematical formulations and their basic principles are explained. A description of different methods, such as the finite-difference, finite-sum, finite-element and boundary-element methods, is presented. The book also presents a way to handle some special boundary value problems, nonlinearities, and eddy currents resulting from the motion, and explains how to understand the effects by means of pre- and post-processing.

For time dependent eddy-current problem with arbitrary external connection, the stability of the time-stepping finite-element method was examined by Tsukerman (1995). He found that the backward Euler method is stable, while the Crank-Nicolson method generates undamped or in some cases even divergent oscillation.

To solve the multi-conductor eddy-current problems in the windings of electrical machines using finite-element analysis, a detailed enough finite-element discretisation is required. As a consequence, the size of the problem increases with an increase in the number of nodes. To cope with the size of the problem, the elimination of the inner nodes from the stator slots was used in the traditional finite-element formulation (Szücs & Arkkio 1999). Szücs (2000) implemented macro-elements in the finite-element analysis (Kladas & Razek 1988a, 1988b) to solve the multi-conductor eddy-current problems. An in-depth literature study regarding multi-conductor eddy-current problems can be found in Szücs (2001). The thesis presented the finite-element formulation of the multi-conductor windings of electrical machines and made a major contribution regarding how to reduce the size of the problem by eliminating the inner nodes from the winding region and combining that with FEA.

Sullivan (2001) presented a squared-field-derivative (SFD) method to calculate the eddy-current loss in round-wire or litz-wire transformer or inductor windings. The method analysed the losses by analytical equation from a two-dimensional or three-dimensional field in multiple windings. However, there were a number of assumptions that limit the scope of the formulation. The method considered only the proximity effect, while the skin effect was neglected by assuming that the wire diameter is smaller than the skin depth. The effect of the parallel windings and their position, which might create circulating currents among the parallel strands, was not considered.

Joksimović & Binder (2003) made an analysis of additional no-load losses resulting from a non-sinusoidal supply in a high-speed cage induction motor. They also built a prototype 16,200-rpm, 270-kW motor to compare the calculated results. Their investigation claims that the eddy-current losses in the stator winding are the main additional loss of an inverter-fed motor. The PWM voltage supply injects voltage harmonics to the motor and causes additional high-frequency current components. In general, these harmonic components increase the additional losses in the stator winding significantly. The authors calculated the effect analytically, as well as numerically. However, the influence of eddy currents in the stator winding was difficult to model, so only the best-case and worst-case situations were considered.

The current distribution and power-loss analysis of the multi-conductor winding of electromagnetic gear was presented by Patecki et al. (2004). The multi-conductor system was modelled by means of 3-D FEM. The differential equations were formulated using a magnetic vector potential and electric scalar potential. The presented results show that the uneven current distribution resulting from the skin effects changes the winding resistances significantly. They proposed dividing the so-called massive conductor into two or four parts to reduce the skin effect. However, the authors did not mention anything about the finite-element discretisation of the windings in their consideration of the skin effects.

Lee et al. (2004) presented the loss distribution of a three-phase induction motor. The motor was supplied from a PWM voltage source. The simulation was performed by the variable time-discretised finite-element method and the results were compared with experimental results. However, the experimental results were only presented for the bar losses in the rotor and the details of the measurements were missing from the article. The stator copper loss was calculated from the current flowing in the wire and its resistance and the stray load losses were assumed to be 1.5% of the motor output (IEEE112). The main focus was on the efficiency of the motor as a result of the PWM supply. The authors compared the results with respect to the sinusoidal supply. Considering the motor efficiency, the authors even recommended not using PWM inverters for driving motors.

Fouladgar & Chauveau (2005) studied the temperature rise in an asynchronous motor as a consequence of the non-sinusoidal voltage supply. The stator and rotor current harmonics were calculated using a time-stepping FEM. The electrical and mechanical losses were introduced into a heat-transfer equation to calculate the temperature distribution. The Fourier decomposition of a particular pulsed-voltage signal was used for comparison with the sinusoidal approximation. They measured the temperature rise in a rotor bar. The temperature was up to 5% higher because of the harmonics presented in the voltage supply. The homogenisation technique was used to consider the loss resulting from eddy currents in random-wound stator windings. However, the eddy-current effect was neglected in the stator field equations.

Zheng et al. (2005) investigated the current distribution in the windings of a four-quadrant transducer (4QT). The 4QT prototype was built for the torque and speed control of the internal combustion engine of hybrid electric vehicles. Because of the high base frequency (300 to 400 Hz) of the transducer, the eddy-current effect in the stator and rotor winding was modelled to calculate the copper losses using 2-D FEM. A commercial FEM software package, *Ansoft*, was used for modelling and simulation.

To consider the skin and proximity effects of multi-turn windings in 2-D finite-element analysis, a frequency-domain homogenisation technique was used (Gyselinck & Dular 2005, Gyselinck & Robert 2005). In the frequency-domain technique, the complex reluctivity tensor was used in the stiffness matrix to consider the proximity effect (Moreau et al. 1998). To consider the skin effect, the DC resistance was replaced by the complex skin effect impedance in an electrical circuit equation related to the winding current and voltage. The frequency-domain technique was extended to the time-domain homogenisation technique (Gyselinck & Robert 2005, Gyselinck et al. 2007). In the time-domain technique, additional induction components were added through magnetic vector potential components in order to take the proximity effect into account. The time-domain skin effect was taken into account by considering the auxiliary currents in the electrical circuit equations. As an example of the applications, the winding of an inductor was modelled using homogenisation techniques (Gyselinck & Dular 2005, Gyselinck & Robert 2005, Gyselinck et al. 2007) in the 2-D finite-element method.

The time-domain homogenisation technique was also used in 3-D finite-element models to consider the eddy-current effect in the core (Gyselinck & Dular 2004) and in the winding (Sabariego et al. 2008) of an inductor. With the homogenisation technique, the eddy-current problem can be solved much more economically with a reasonable mesh size, without fine discretisation of the composite materials (El Feddi et al. 1997).

An efficient harmonic-balance method (HBM) was presented by Ausserhofer et al. (2007) to determine the steady-state solution of non-linear eddy-current problems. A similar kind of approach was also presented by Ciric et al. (2007) using the name ‘efficient harmonic method’. The authors increased the efficiency of the calculation method by combining the HBM (Yamada & Bessho 1988, Yamada et al. 1989) and the fixed point method (Bíró & Preis 2006). To further improve its efficiency, Ciric et al. (2007) restricted the number of harmonics so that it was low and added more harmonics only if needed. The harmonic-balance method was combined with FEM and named as the so-called *harmonic-balance finite-element method*. The vector potentials, flux densities, applied currents, and magnetic reluctivities are approximated as harmonic solutions and solved as nonlinear eddy current problems (Yamada et al. 1991). By using this method, saturation and hysteresis (Lu et al. 1990), as well as motion and external circuit (Lu et al. 1991), were taken into account.

To determine the eddy currents and losses in large axi-symmetric filter air coils built with a special type of turn, a finite-element method based procedure was presented by Preis et al. (2008). To take into account the non-uniform current distribution between the different layers by retaining the axi-symmetry, they used a one-component vector potential combined with circuit equation. They proposed a simplified method to take into account the parallel stranding of the wires. The proposed method neglected the circulating currents between the parallel strands. The wires in the cable were stranded in layers only. A simplified scheme for the cross-section of the cable was also introduced to reduce the number of finite elements.

Conclusion of the literature study

The survey of the published literature has indicated that the eddy-current problem in the multi-conductor winding of electrical machines is very important. The recent trend and applications towards inverter-driven motors increases the importance of the problem further. Most of the recent relevant works were subjected to reduce the computational time and memory requirement. There are several formulations to handle the large numerical problem more economically. Before those formulations, some authors developed methods restricted to a couple of conductors only. Clearly, there is a lack of a comprehensive method or simulation tool to analyse the effects of eddy currents and circulating currents in the multi-conductor windings of electrical machines. In most of the available simulation tools, these effects are neglected from the field equation and considered as post-processing or neglected totally considered as insignificant effects.

3 Methods

3.1 Overview of the electromagnetic field

The time variation of the magnetic field induces eddy currents in a conducting material. The phenomenon can be realised from the law of Faraday (Eq. 3). The assumptions used to consider eddy currents in the windings of electrical machines with 2-D finite-element analysis (FEA) are not different from the most common assumptions used when investigating electrical machinery. In this case, the modified Maxwell's field equations can be represented as (Chari & Silvester 1980, Krawczyk & Tegopoulos 1993)

$$\nabla \times \boldsymbol{E} = -\frac{\partial \boldsymbol{B}}{\partial t} \tag{3}$$

$$\nabla \times \boldsymbol{H} = \boldsymbol{J} \tag{4}$$

$$\boldsymbol{J} = \sigma \boldsymbol{E} \tag{5}$$

$$\boldsymbol{B} = \mu \boldsymbol{H} \tag{6}$$

where $\boldsymbol{E}$ is the electric field strength
$\boldsymbol{B}$ is the magnetic flux density
t is the time
$\boldsymbol{H}$ is the magnetic field strength
$\boldsymbol{J}$ is the current density
μ is the permeability of the material
σ is the conductivity of the material

There are three potential formulations in electromagnetic field analysis (Demenko 2006):

a) Magnetic scalar-electric vector potential (Ω-$\boldsymbol{T}$)

b) Magnetic - electric vector potential ($\boldsymbol{A}$-$\boldsymbol{T}$)

c) Magnetic vector potential – electric scalar potential ($\boldsymbol{A}$-φ).

In the dissertation the $\boldsymbol{A}$-φ formulation is used which is well adopted for 2D problems.

The magnetic vector potential is defined as

$$\boldsymbol{B} = \nabla \times \boldsymbol{A} \tag{7}$$

The electric scalar potential ϕ can be obtained from Eqs. (3) and (7)

$$\boldsymbol{E} = -\frac{\partial \boldsymbol{A}}{\partial t} - \nabla \phi \tag{8}$$

In the quasi-static case, the magnetic vector potential $\boldsymbol{A}$ is

$$\nabla \times (\frac{1}{\mu} \nabla \times \boldsymbol{A}) = \boldsymbol{J} \tag{9}$$

The current density is given by

$$\boldsymbol{J} = -\sigma \frac{\partial \boldsymbol{A}}{\partial t} - \sigma \nabla \phi \tag{10}$$

The divergence of the current density satisfy the condition

$$\nabla \cdot \boldsymbol{J} = 0 \tag{11}$$

The equations for the vector and scalar potentials are obtained by substituting Eq. (10) in Eq. (9)

$$\nabla \times (\frac{1}{\mu} \nabla \times \boldsymbol{A}) + \sigma \frac{\partial \boldsymbol{A}}{\partial t} + \sigma \nabla \phi = 0 \tag{12}$$

More details can be found in Arkkio (1987) and Szücs (2001).

3.2 Basic equations

3.2.1 Electromagnetic field

The basic equation governing the electromagnetic field in the 2-D model (Yatchev 1995, Islam et al. 2007, Islam & Arkkio 2009a, Islam & Arkkio 2009b) is

$$\nabla \times (\nu \nabla \times \boldsymbol{A}) + \sigma \frac{\partial \boldsymbol{A}}{\partial t} - \left(\frac{1}{l_{\mathrm{e}}} \sum_{j=1}^{Q_{\mathrm{b}}} \sigma \eta_j u_j^{\mathrm{b}} \right) \boldsymbol{e_z} = 0 \tag{13}$$

where $\boldsymbol{A}$ is the magnetic vector potential having only one non-zero component. In 2D FEM, it is represented by $\boldsymbol{A} = \boldsymbol{e_z} A_{\mathrm{z}}$, ν is the reluctivity, l_{e} is the effective length of the machine, Q_{b} is the number of bars of the winding in the solution region, and η_j is a function to relate the nodal point of bar *j*

$$\eta_j = \begin{cases} 1 & \text{if the point belongs to bar } j \\ 0 & \text{otherwise} \end{cases}$$

u_j is the potential difference of bar *j*.

3.2.2 Form-wound multi-phase winding

The voltage equation of a bar is

$$u_n^{\mathrm{b}} = R_{\mathrm{b}} \sum_{j=1}^{Q_m} \eta_{nj} i_j + R_{\mathrm{b}} \int_{S_n} \sigma \frac{\partial \boldsymbol{A}}{\partial t} \cdot \mathrm{d}\boldsymbol{S_n} \qquad ; n = 1, ..., Q_{\mathrm{b}} \tag{14}$$

where, R_{b} is the DC resistance of a bar of length l_{e}, Q_m is the number of phases, and η_{nj} is the function to relate between the bar *n* and phase *j*

$$\eta_{nj} = \begin{cases} 1 & \text{if bar } n \text{ belongs to a positive coil side of phase } j \\ -1 & \text{if bar } n \text{ belongs to a negative coil side of phase } j \\ 0 & \text{otherwise} \end{cases}$$

S_n is the cross-sectional area of the n^{th} bar of the winding.

The voltage equation of a phase is

$$u_m = Q_{\text{ss}} \sum_{j=1}^{Q_{\text{b}}} \eta_{jm} u_j^{\text{b}} + L_{\text{e}} \frac{\mathrm{d}i_m}{dt} + R_{\text{e}} i_m \qquad ; m = 1, \ldots, Q_m \tag{15}$$

where Q_{ss} is the number of symmetry sectors, i_m is the phase current of the m^{th} phase, R_{e} is the end-winding DC resistance of a phase, and L_{e} is the end-winding inductance of a phase. The bar equation is strongly coupled with the field and phase equations. For a cage induction motor, the form-wound phase winding is present only in the stator. The rotor cage is a special form of winding that can be modelled with a voltage equation of bar, and, instead of the phase equation, the equation for the end rings that connects the parallel rotor bars (Arkkio 1987, Islam et al. 2007, Islam & Arkkio 2009a).

3.3 Numerical discretisation

3.3.1 Finite-element discretisation

The fundamental idea of finite-element analysis (FEA) is to subdivide the region into small sub-regions called finite elements. To model the eddy currents and circulating currents in the windings with FEA, all the stator bars connected in series and parallel should be considered. As a result, finite-element discretisation of every bar is an essential requirement. To take the effects of eddy currents into account accurately, a detailed enough finite-element discretisation of the bar is required (Reichert et al. 1988).

3.3.2 Time-dependence

The time-dependent field equations have to be solved by discretisation in time, in addition to spatial discretisation. The analysis can be greatly simplified if the field varies sinusoidally in time. In this case, the time dependence can be eliminated from the equations by using complex field quantities. In a 2D case, the vector potential and current density are

$$\begin{aligned} \boldsymbol{A} &= \mathrm{Re}\{\underline{A}(x,y)\mathrm{e}^{\mathrm{j}\omega t}\}\boldsymbol{e}_z \\ \boldsymbol{J} &= \mathrm{Re}\{\underline{J}(x,y)\mathrm{e}^{\mathrm{j}\omega t}\}\boldsymbol{e}_z \end{aligned} \tag{16}$$

where ω is the angular frequency of the time variation. The assumption of sinusoidal time variation is valid only in a steady state for a linear system without motion. In a real electrical machine, a sinusoidally time-varying source does not induce a sinusoidally-varying magnetic field. However, to simplify the solution procedure, the sinusoidal approximation is often also used for non-linear cases. A detailed derivation of the basic equations with sinusoidal approximation to the matrix form of equations of a cage induction motor can be found in Islam et al. (2007).

In a non-linear system, the true time-dependence can be solved by a time-discretised finite-element method. A generalised first-order finite difference procedure is used for the time-stepping. If k and $k+1$ denote two successive instants of time, the vector potential and phase current at the $(k+1)^{\text{th}}$ instant of time are

$$\boldsymbol{A}_{k+1} = \boldsymbol{A}_k + \left[\beta \left. \frac{\partial \boldsymbol{A}}{\partial t} \right|_{k+1} + (1-\beta) \left. \frac{\partial \boldsymbol{A}}{\partial t} \right|_{k} \right] \Delta t \tag{17}$$

$$i_{k+1} = i_k + \left[\beta \left. \frac{\partial i}{\partial t} \right|_{k+1} + (1-\beta) \left. \frac{\partial i}{\partial t} \right|_{k} \right] \Delta t \tag{18}$$

where Δt is the length of the time step and β is a weighting parameter between 0 and 1. The three most popular values used for β are: 0 – direct Euler method; 0.5 – Crank-Nicolson (trapezoidal) method, and 1 – Backward Euler method (Yatchev 1995, Islam & Arkkio 2008a).

3.3.3 Modelling of motion

The equations of the stator and rotor fields are written in their own coordinate systems. The solutions of the two field equations are forced to be continuous over the air gap. The rotor is rotated at each time step through an angle corresponding to the mechanical angular frequency. The finite elements in the air gap are modified to allow the continuous motion of the rotor (Davat et al. 1985, Arkkio 1990). The Galerkin method is applied to the basic equations and formulated to a matrix form of the global system of equations. A detailed enough finite-element discretisation is considered in the slot region to consider eddy and circulating currents. The Crank-Nicolson method is found to be unstable when considering eddy currents in the winding and the Backward Euler method (β=1) is used to discretise the equations of the machine in time.

3.3.4 Matrix form of equations

The system of equations is solved by the Newton-Raphson method for the i^{th} non-linear iteration. At a certain time step k+1, the system of equations for the cage induction motor is

$$\begin{bmatrix} \boldsymbol{P}\left(a_{k+1}^{(i)}\right) & (\boldsymbol{D}^{\mathrm{r}})^{\mathrm{T}} & \boldsymbol{0} & (\boldsymbol{D}^{\mathrm{s}})^{\mathrm{T}} \\ \boldsymbol{D}^{\mathrm{r}} & \boldsymbol{C}_{\mathrm{b}}^{\mathrm{r}} & \boldsymbol{0} & \boldsymbol{0} \\ \boldsymbol{0} & \boldsymbol{0} & \boldsymbol{C}^{\mathrm{s}} & \boldsymbol{K}(\boldsymbol{G}^{\mathrm{s}})^{\mathrm{T}} \\ \boldsymbol{D}^{\mathrm{s}} & \boldsymbol{0} & \boldsymbol{G}^{\mathrm{s}}(\boldsymbol{K})^{\mathrm{T}} & \boldsymbol{C}_{\mathrm{b}}^{\mathrm{s}} \end{bmatrix} \begin{bmatrix} \Delta\boldsymbol{a}_{k+1}^{(i)} \\ \Delta\boldsymbol{u}_{p_{k+1}}^{\mathrm{r}(i)} \\ \Delta\boldsymbol{i}_{m_{k+1}}^{\mathrm{s}(i)} \\ \Delta\boldsymbol{u}_{n_{k+1}}^{\mathrm{s}(i)} \end{bmatrix} = - \begin{bmatrix} \boldsymbol{f}^{a}(\boldsymbol{a}_{k+1}^{(i)}, \boldsymbol{u}_{p_{k+1}}^{\mathrm{r}(i)}, \boldsymbol{u}_{n_{k+1}}^{\mathrm{s}(i)}) \\ \boldsymbol{f}_{p}^{\mathrm{r}}(\boldsymbol{a}_{k+1}^{(i)}, \boldsymbol{u}_{p_{k+1}}^{\mathrm{r}(i)}) \\ \boldsymbol{f}_{m}^{\mathrm{s}}(\boldsymbol{i}_{m_{k+1}}^{\mathrm{s}(i)}, \boldsymbol{u}_{m_{k+1}}^{\mathrm{ph}(i)}) \\ \boldsymbol{f}_{n}^{\mathrm{s}}(\boldsymbol{a}_{k+1}^{(i)}, \boldsymbol{i}_{m_{k+1}}^{\mathrm{s}(q)}, \boldsymbol{u}_{n_{k+1}}^{\mathrm{s}(i)}) \end{bmatrix} \quad (19)$$

A detailed derivation of the basic equations with time-harmonic FEA to the matrix form of equations (Eq. 19) can be found in Islam et al. (2007) and with time-discretised FEA in Yatchev et al. (1995) and Islam & Arkkio (2008a).

The system of equations for the DFIG is (Islam & Arkkio 2009):

$$\begin{bmatrix} \boldsymbol{P}\left(a_{k+1}^{(i)}\right) & \boldsymbol{0} & (\boldsymbol{D}^{\mathrm{r}})^{\mathrm{T}} & \boldsymbol{0} & (\boldsymbol{D}^{\mathrm{s}})^{\mathrm{T}} \\ \boldsymbol{0} & \boldsymbol{C}^{\mathrm{r}} & \boldsymbol{K}(\boldsymbol{G}^{\mathrm{r}})^{\mathrm{T}} & \boldsymbol{0} & \boldsymbol{0} \\ \boldsymbol{D}^{\mathrm{r}} & \boldsymbol{G}^{\mathrm{r}}(\boldsymbol{K})^{\mathrm{T}} & \boldsymbol{C}_{\mathrm{b}}^{\mathrm{r}} & \boldsymbol{0} & \boldsymbol{0} \\ \boldsymbol{0} & \boldsymbol{0} & \boldsymbol{0} & \boldsymbol{C}^{\mathrm{s}} & \boldsymbol{K}(\boldsymbol{G}^{\mathrm{s}})^{\mathrm{T}} \\ \boldsymbol{D}^{\mathrm{s}} & \boldsymbol{0} & \boldsymbol{0} & \boldsymbol{G}^{\mathrm{s}}(\boldsymbol{K})^{\mathrm{T}} & \boldsymbol{C}_{\mathrm{b}}^{\mathrm{s}} \end{bmatrix} \begin{bmatrix} \Delta\boldsymbol{a}_{k+1}^{(i)} \\ \Delta\boldsymbol{i}_{p_{k+1}}^{\mathrm{r}(i)} \\ \Delta\boldsymbol{u}_{q_{k+1}}^{\mathrm{r}(i)} \\ \Delta\boldsymbol{i}_{m_{k+1}}^{\mathrm{s}(i)} \\ \Delta\boldsymbol{u}_{n_{k+1}}^{\mathrm{s}(i)} \end{bmatrix} = - \begin{bmatrix} \boldsymbol{f}^{a}(\boldsymbol{a}_{k+1}^{(i)}, \boldsymbol{u}_{p_{k+1}}^{\mathrm{r}(i)}, \boldsymbol{u}_{n_{k+1}}^{\mathrm{s}(i)}) \\ \boldsymbol{f}_{p}^{\mathrm{r}}(\boldsymbol{i}_{p_{k+1}}^{\mathrm{r}(i)}, \boldsymbol{u}_{p_{k+1}}^{\mathrm{r^L}(i)}) \\ \boldsymbol{f}_{q}^{\mathrm{r}}(\boldsymbol{a}_{k+1}^{(i)}, \boldsymbol{i}_{p_{k+1}}^{\mathrm{r}(i)}, \boldsymbol{u}_{q_{k+1}}^{\mathrm{r}(i)}) \\ \boldsymbol{f}_{m}^{\mathrm{s}}(\boldsymbol{i}_{m_{k+1}}^{\mathrm{s}(i)}, \boldsymbol{u}_{m_{k+1}}^{\mathrm{s^L}(i)}) \\ \boldsymbol{f}_{n}^{\mathrm{s}}(\boldsymbol{a}_{k+1}^{(q)}, \boldsymbol{i}_{m_{k+1}}^{\mathrm{s}(i)}, \boldsymbol{u}_{n_{k+1}}^{\mathrm{s}(i)}) \end{bmatrix} \quad (20)$$

where $\boldsymbol{P}\left(a_{k+1}^{(i)}\right)$ is the sub-matrix of the Jacobian matrix related to the nodal values of the vector potentials, $(\boldsymbol{D}^{\mathrm{r}})^{\mathrm{T}}$ and $(\boldsymbol{D}^{\mathrm{s}})^{\mathrm{T}}$ are the sub-matrices related to the bar voltages of the rotor and stator of the field equation. $\boldsymbol{D}^{\mathrm{r}}$, $\boldsymbol{C}^{\mathrm{r}}$, $\boldsymbol{K}(\boldsymbol{G}^{\mathrm{r}})^{\mathrm{T}}$, $\boldsymbol{G}^{\mathrm{r}}(\boldsymbol{K})^{\mathrm{T}}$, and $\boldsymbol{C}_{\mathrm{b}}^{\mathrm{r}}$ are the sub-matrices related to the rotor circuits. $\boldsymbol{D}^{\mathrm{s}}$, $\boldsymbol{C}^{\mathrm{s}}$, $\boldsymbol{K}(\boldsymbol{G}^{\mathrm{s}})^{\mathrm{T}}$, $\boldsymbol{G}^{\mathrm{s}}(\boldsymbol{K})^{\mathrm{T}}$, and $\boldsymbol{C}_{\mathrm{b}}^{\mathrm{s}}$ are the sub-matrices related to the stator circuits. $\Delta\boldsymbol{a}_{k+1}^{(i)}$, $\Delta\boldsymbol{i}_{p_{k+1}}^{\mathrm{r}(i)}$, $\Delta\boldsymbol{u}_{q_{k+1}}^{\mathrm{r}(i)}$, $\Delta\boldsymbol{i}_{m_{k+1}}^{\mathrm{s}(i)}$ and $\Delta\boldsymbol{u}_{n_{k+1}}^{\mathrm{s}(q)}$ are the increments of the vector potential nodal values, rotor phase currents, potential differences of the rotor bars, phase currents, and potential differences of the stator bars, respectively.

A more detailed description can be found in Arkkio (1987), Islam & Arkkio (2008a), and Islam & Arkkio (2009).

3.4 Equations for loss analysis

3.4.1 Resistive losses

The resistive stator losses in the part of the stator winding embedded in the slots (Yatchev 1995, Islam et al. 2007) is

$$P_{\mathrm{sb}}^{\mathrm{s}} = \frac{Q_{\mathrm{ss}} l_{\mathrm{e}}}{\sigma} \sum_{i=1}^{Q_{\mathrm{b}}^{\mathrm{s}}} \int_{\Omega} \eta_i^{\mathrm{s}} \boldsymbol{J}^2 \mathrm{d}\Omega \tag{21}$$

where the total current density in the stator bar i is

$$\boldsymbol{J} = -\sigma \frac{\partial \boldsymbol{A}}{\partial t} + \sigma \frac{u_i^{\mathrm{s}}}{l_{\mathrm{e}}} \boldsymbol{e_z} \tag{22}$$

The end-winding resistive loss has been calculated from the DC resistance of the end winding and phase current

$$P_{\mathrm{ew}}^{\mathrm{s}} = \sum_{i=1}^{Q_m} R_{\mathrm{e}}^{\mathrm{s}} (i_i^{\mathrm{s}})^2 \tag{23}$$

The total resistive loss of the stator winding is

$$P_{\mathrm{t}}^{\mathrm{s}} = P_{\mathrm{sb}}^{\mathrm{s}} + P_{\mathrm{ew}}^{\mathrm{s}} \tag{24}$$

Similarly, for the resistive losses in the part of the rotor winding embedded in the rotor slots of a DFIG

$$P_{\mathrm{sb}}^{\mathrm{r}} = \frac{Q_{\mathrm{ss}} l_{\mathrm{e}}}{\sigma} \sum_{i=1}^{Q_{\mathrm{b}}^{\mathrm{r}}} \int_{\Omega} \eta_i^{\mathrm{r}} \boldsymbol{J}^2 d\Omega \tag{25}$$

where the total current density in the rotor bar i is

$$\boldsymbol{J} = -\sigma \frac{\partial \boldsymbol{A}}{\partial t} + \sigma \frac{u_i^{\mathrm{r}}}{l_{\mathrm{e}}} \boldsymbol{e_z} \tag{26}$$

The formulation for the resistive loss calculation of the rotor cage can be found in Arkkio (1987) and Islam & Arkkio (2008b).

3.4.2 *Eddy-current loss*

The difference between the total resistive loss and the DC resistive loss, calculated from the total DC phase resistance R^{s} and phase current, is the total eddy-current loss of the stator winding

$$P_{\mathrm{eddy}} = P_{\mathrm{t}} - \sum_{i=1}^{Q_m} R^{\mathrm{s}} (i_i^{\mathrm{s}})^2 \tag{27}$$

The eddy-current losses in the rotor winding are calculated in exactly the same way as for the stator winding. For the cage rotor, the resistive losses in the rotor bars are mainly caused by currents induced because of electromagnetic field and considered as eddy-current losses.

3.4.3 Eddy factor

The eddy-current loss arises as a result of the non-uniform current distribution in the bars. This causes the effective resistance to exceed its DC value (Lammeraner 1966). The DC resistance means the resistance calculated from the DC voltage and current. This effective resistance is defined as AC resistance (Silvester 1967, Szücs 2001, Islam et al. 2007). The eddy factor (k_{eddy}) is defined as the ratio between the AC and DC resistance (Salon et al. 1993), which is obtained from the resistive losses

$$k_{\mathrm{eddy}} = \frac{P_{\mathrm{sb}}}{i^2 R_{\mathrm{DC}}} = \frac{i^2 R_{\mathrm{AC}}}{i^2 R_{\mathrm{DC}}} = \frac{R_{\mathrm{AC}}}{R_{\mathrm{DC}}} \tag{28}$$

The eddy factor in Eq. (28) is calculated for the slot embedded part of the winding. As a result, R_{AC} and R_{DC} used in this equation represent the resistances for the slot embedded part of the winding, only.

3.4.4 Circulating-current loss

A circulating current is the difference between the instantaneous average current of the strands and a particular strand current (Lähteenmäki 2002, Islam & Arkkio 2008a). The circulating-current loss is the difference between the total resistive loss of the winding and the ideal resistive loss, assuming that every strand has the same current flowing through it (Lähteenmäki 2002, Islam & Arkkio 2006, Islam & Arkkio 2007). To take into account the circulating current between the parallel strands in the phases, each parallel strand is modelled using Eq. (15). A new sub-indexing of the phases is created. The supply voltage is identical for the parallel strands belonging to a phase but different currents are produced because of the different strand positions in the slots. Mathematically, the circulating-current loss (P_{cc}) can be represented as

$$P_{\mathrm{cc}} = \sum_{i=1}^{m} \left(\sum_{j=1}^{N} \left(R_{ij}^{\mathrm{str}} \cdot \left| I_{ij}^{\mathrm{str}} \right|^2 \right) - R_i \left| I \right|^2 \right) \tag{29}$$

where m is the number of phases, N is the number of parallel strands in one phase, R_{ij}^{str} is the DC resistance of strand j of phase i, I_{ij}^{str} is the rms current in strand j of phase i, R_i is the DC phase resistance, and I is the total rms current in phase i.

4 Results

4.1 Cage induction motor

4.1.1 Simulated motor

A 1250-kW, 3-phase, 50-Hz, 690-V, delta-connected cage induction motor is considered. Table 1 provides the data of the motor.

Table 1: Data of the machine that was studied

Number of pole pairs	3
Number of parallel branches	3
Number of parallel strands in a coil	3
Number of stator slots	72
Number of rotor slots	86
Number of teeth in a coil pitch	10
Inner diameter of the stator core (mm)	670
Outer diameter of the rotor core (mm)	663
Effective length of the machine (mm)	810
Rated slip (%)	0.365

The winding arrangement of a phase with transposition is presented in Figure 1. A bar is defined as that part of a strand that is embedded in a slot. The bars are connected in series in a particular strand. Same colour bars belong to a strand (Figure 1) and they are connected in series. There are 3 parallel connected copper strands (red, green and blue), which together make an effective turn. There are 6 effective turns, which results in 18 bars per slot. For a double-layer winding, every coil side consists of 3 effective turns. The coil pitch is 10 slot pitches. Thus, the coils are chorded 5/6 to reduce the harmonic contents. Every bar of the stator is modelled separately and the connection matrices are introduced to make a strong coupling with those bars to a particular strand which belongs to a particular phase, as well as to the field equation. The stator bars were transposed systematically from one coil to the next one in order to minimise the circulating currents among the parallel strands (Islam et al. 2007, Islam & Arkkio 2008a).

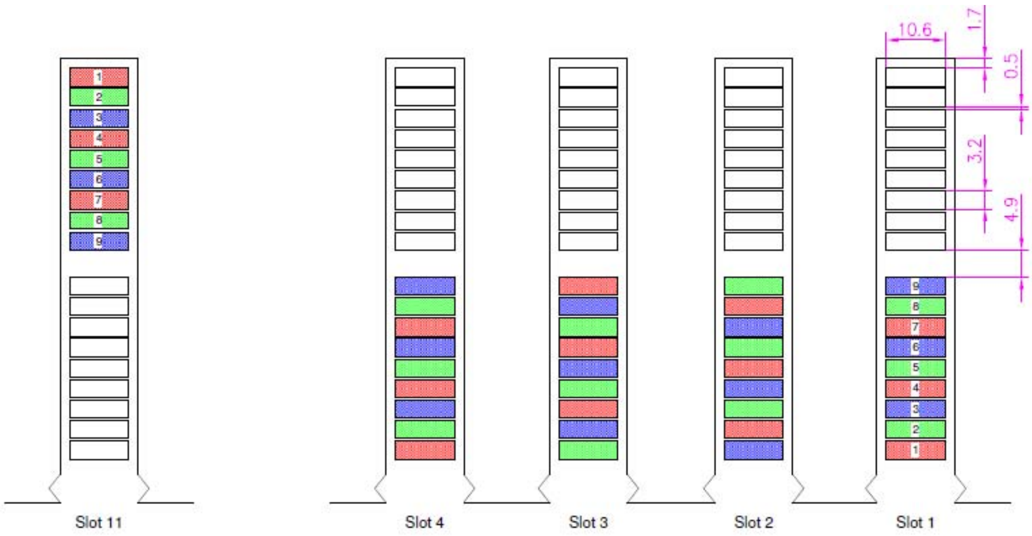

Figure 1: Winding arrangement of a phase of the motor.

A second-order isoparametric finite-element discretisation is used to simulate the electrical machine. The finite-element discretisation of the stator conductor region when the number of elements in a bar is 4 is presented in Figure 2a and when the number of elements in a bar is 8 in Figure 2b. The dimensions and numbering of the stator bars in a slot are presented in Figure 2c. The accuracy of the finite-element discretisation is analysed in Section 4.1.6. Figures 2a and 2b are selected based on this analysis. Using the symmetry, only a half of the electrical machine is solved with the finite-element solver.

The flux-density distribution of the computed region is presented in Figure 3 using magnetic equipotential lines at the rated load. The time-discretised FEM model required 6.4 hours of CPU time to simulate a 0.4-second transient time using a 0.05-ms time-step size. There were 43 557 nodes in the FE model. A Pentium 4, dual core 2.6 GHz computer was used for the simulation. When modelling the laminated cores of the electrical machines, magnetisation curves and loss data from EN 10106:2007 M400-50A grade steel sheets were used. In the time harmonic calculation, a modified B-H curve is used (Arkkio 1987, Eq. (47)).

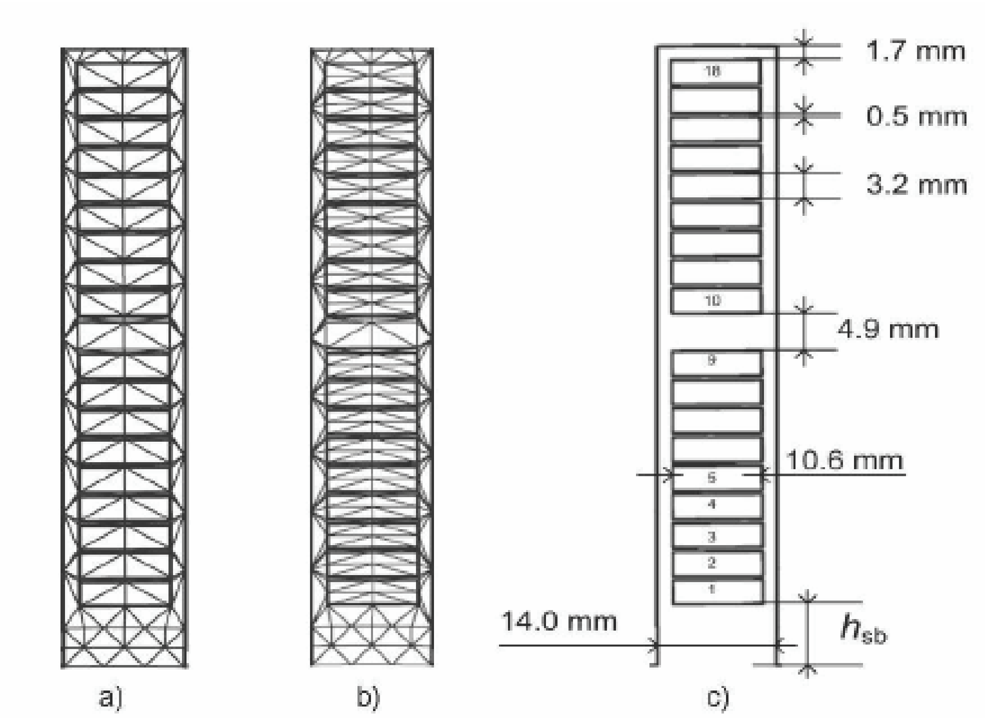

Figure 2: The conductors in the stator slot: a) 4 finite elements in a bar, b) 8 finite elements in a bar, and c) dimensions and numbering of the stator bars in a slot.

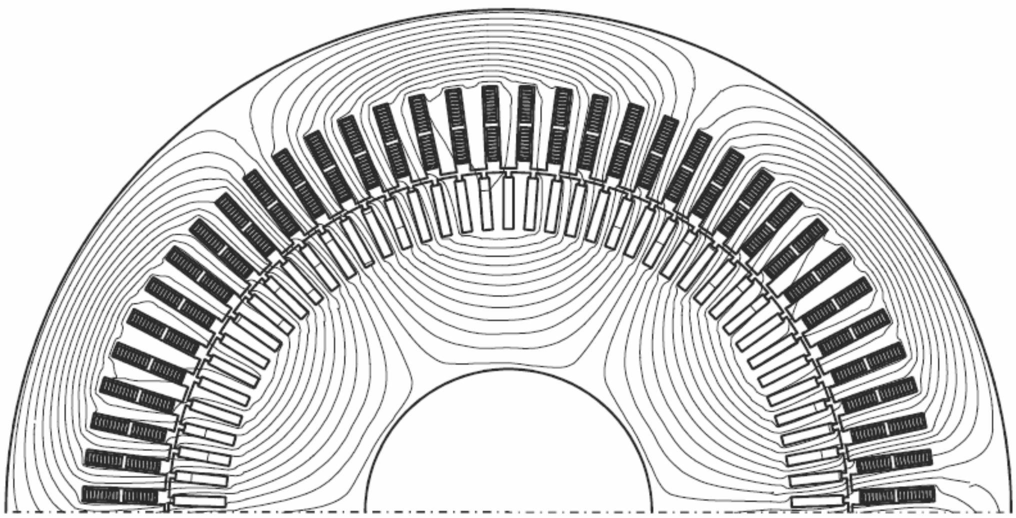

Figure 3: The flux-density distribution is presented using magnetic equipotential lines.

4.1.2 Voltage supply

The motor is supplied from a voltage source. In time-harmonic finite-element analysis, only a sinusoidal voltage source is used. In time-discretised analysis, in addition to the sinusoidal supply, the PWM voltage supply is used as a non-sinusoidal supply source for the motor. The PWM supply is obtained by applying sinus-triangle comparison. A third harmonic is injected into the sinusoidal modulating signal to increase the fundamental harmonic and to reduce the harmonic contents (Grant et al 1985, Holmes & Lipo 2003, Meco-Gutiérrez et al. 2007) from the PWM supply. The switching frequency (the triangle carrier frequency) of the PWM supply is 2 kHz for the simulations. A higher switching frequency in the frequency-converter supply may require a shorter time step compared to the one used for sinusoidal supply.

4.1.3 Position of the conductors in a slot

The radial distance of the stator bars from the inner surface of the stator, i.e. the outer surface of the air gap, is one of the very important design parameters regarding losses (Oberretl 1969), especially the eddy-current losses of the stator winding. The radial position of the coil sides is changed by increasing the distance from the inner surface of the stator to the top of the stator bar, h_{sb}, from 0.8 mm to 25.8 mm by increasing the stator slot height from 73.0 mm to 98 mm. The outer diameter of the machine is increased to keep the thickness of the yoke constant. The constant distance (1.7 mm) from the bottom of the stator bars to the bottom of the slot is maintained throughout all of the simulations (Figure 2c). Changing the geometry changes the leakage flux. The input voltage is adjusted to keep the fundamental harmonic of the air-gap flux density constant (0.711 T). A rectangular and fully open stator slot geometry with a non-magnetic wedge (Figure 2) is used for the simulations (Islam et al. 2007, Islam & Arkkio 2008a, Islam & Arkkio 2009a).

To investigate the effects of the radial position of the stator bars, eddy-current effects are presented in Figure 4 as a function of h_{sb} for a sinusoidal supply with time-harmonic and time-stepping analysis. To study the effects of a PWM supply, the eddy-current effect is also presented in the same figure (Figure 4) as a function of h_{sb} for the PWM supply. The effect of the PWM supply is studied with time-discretised finite-element analysis only. The eddy-current effect $(k_{eddy} - 1)$ is defined as the relative difference between the AC and DC resistance ($R_{AC}/R_{DC} - 1$) (Islam et al. 2007, Islam & Arkkio 2008a, Islam & Arkkio 2009a).

For the sinusoidal supply, a distance of the stator bars from the inner surface of the stator that is greater than 7.0 mm eliminates most of the eddy-current losses that it is possible to reduce by adjusting the position of the coils. A small improvement is possible until 14.0 mm, but after that the eddy-current loss remains constant. For the PWM supply, the small improvement seems continuous after 7.0 mm.

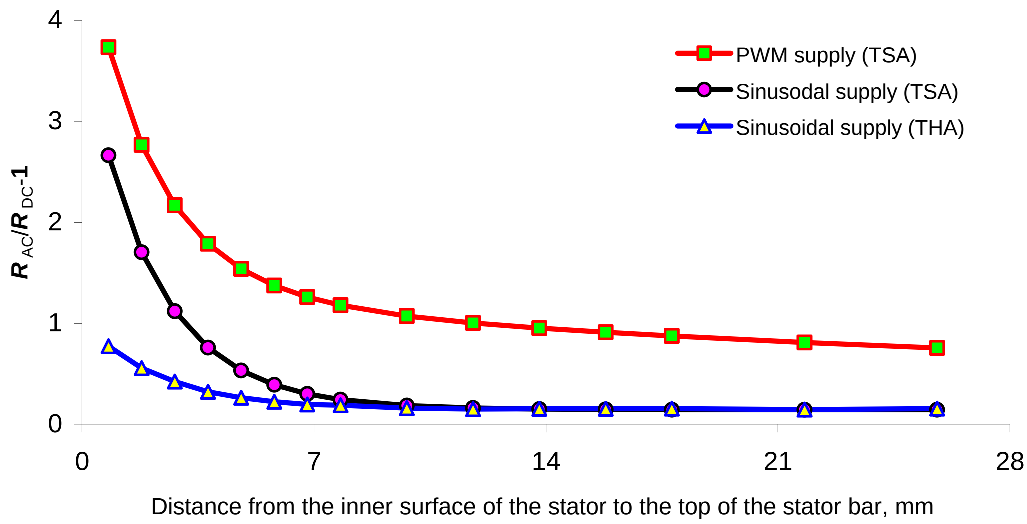

Figure 4: Eddy-current effects as a function of the distance from the inner surface of the stator to the top of the stator bar, h_{sb}, for the PWM and sinusoidal supplies. For the sinusoidal supply, both the time-harmonic analysis (THA) and time-stepping analysis (TSA) are considered. For all those cases, the stator winding is transposed and the fundamental harmonic air-gap flux density is 0.711 T.

When the machine is supplied from a sinusoidal voltage source, the main source of eddy-current losses in the stator winding is the rotor-slot harmonics acting in the region close to the tooth tips. When increasing the distance, h_{sb}, the conductors are removed from the active zone of the rotor-slot harmonics, and the losses caused by the slot harmonics vanish.

When the machine is supplied from a PWM voltage, a significant part of the eddy-currents are generated by the high-frequency flux associated with the non-sinusoidal supply. When increasing the distance h_{sb}, the leakage inductance of the slot increases, and the harmonic stator currents and the high-frequency flux in the conductor region decrease. However, they never vanish completely from the stator conductors.

The different behaviours of these two main sources of losses explain the differences in the losses observed as functions of the parameter h_{sb}. However, for any kind of supply, the situation can be disastrous if the stator coils are placed very close to the air gap. At small values of h_{sb}, the rotor-slot harmonics generate significant losses in the stator bars. This effect is relatively independent of the supply modes. The result presented in Figure 3 is based on the results in publications P1, P2, and P3. By using the magnetic slot wedge, the eddy-current loss of the stator winding can be reduced. The effect of magnetic slot wedges on the eddy currents is studied in publications P1-P3. The magnetic slot wedges are commonly used in cage induction machines with form-wound stator windings.

A thermal analysis was performed by Prof. Arkkio, using the public domain software FEMM (Meeker 2009) to study the possible hot spots of the stator winding. Figure 5 presents the temperature rise of a slot when the motor is supplied from a PWM voltage supply and the distance from the inner surface of the stator to the top of the stator bar, h_{sb}, is equal to 7.8 mm. The maximum and average temperature rise of the slot-embedded stator winding is presented as a function of h_{sb} in Figure 6. The maximum temperature, i.e. hot spot is always in the top most bars of the slots.

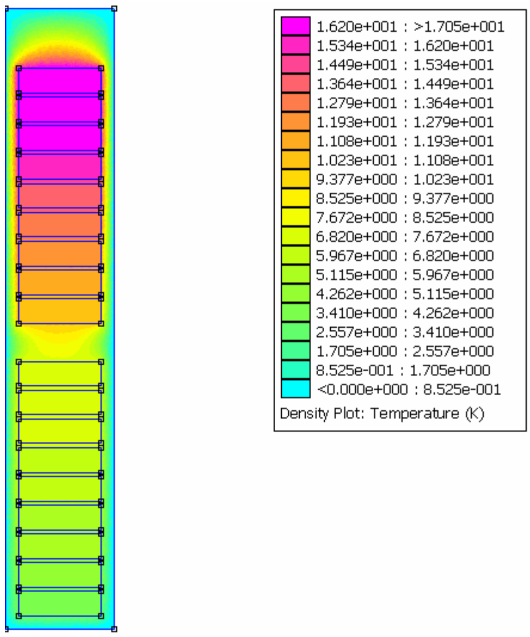

Figure 5: Temperature rise distribution of the stator bars in a slot when the motor is supplied from a PWM voltage source. The distance from the inner surface of the stator to the top of the stator bar, h_{sb}, is equal to 7.8 mm.

The results of the 2-D thermal analysis indicate that the temperature rise can be dangerous if the stator winding is very close to the air gap. The analysis is performed on the basis of the average loss density of each stator bar. The losses are obtained from the finite-element analysis of the 1250-kW motor (Table 1) after considering the eddy currents in the stator winding. A constant temperature boundary condition is assumed for the iron core. The heat conductivity of the insulation layer is $0.25\ \mathrm{W/mK}$ and the heat-transfer coefficient at the air surface at the slot opening is $35\ \mathrm{W/m^2K}$ (Saari 1998).

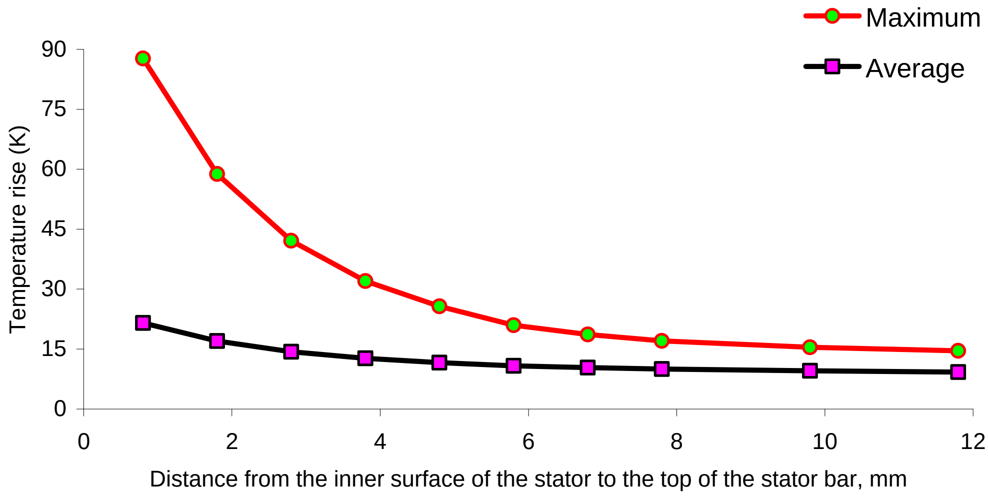

Figure 6: The maximum and average temperature rise in the stator slot is presented as a function of the distance from inner surface of the stator to the top of the stator bar, h_{sb} . The motor is supplied from PWM voltage source.

4.1.4 Circulating currents and transposition

A circulating current is the difference between the average current of the strands and a particular strand current (Lähteenmäki 2002, Takahashi et al. 2003). The systematic transposition of the stator bars is a well-known solution for the reduction of the circulating currents and their losses (Bennington et al. 1970, Baodong et al. 1995, Dexin et al. 2000, Haldemann 2004). To observe the phenomenon, the currents in all the three parallel strands of 'phase A' are plotted as a function of time for the sinusoidal supply. Figure 7 presents the strand currents without any transposition. Figure 8 presents the strand currents when the stator bars are transposed systematically (Islam & Arkkio 2008a). The circulating currents can be reduced practically to zero using the systematic transposition of the stator bars. However, it may be difficult to use such slot numbers and bar numbers as would allow the perfect transposition.

Without transposition, the rms current is higher in one strand and lower in another strand by about 14%. As a consequence, the total resistive loss of the stator winding remains almost the same with and without the transpositions. Because of this higher strand current of 'A1', the loss in this strand is 30.6% higher than the average losses of the strands. This would overheat the strand. With the PWM supply, the percentage of loss increase for a particular strand compared to the average value is similar to that with the sinusoidal supply.

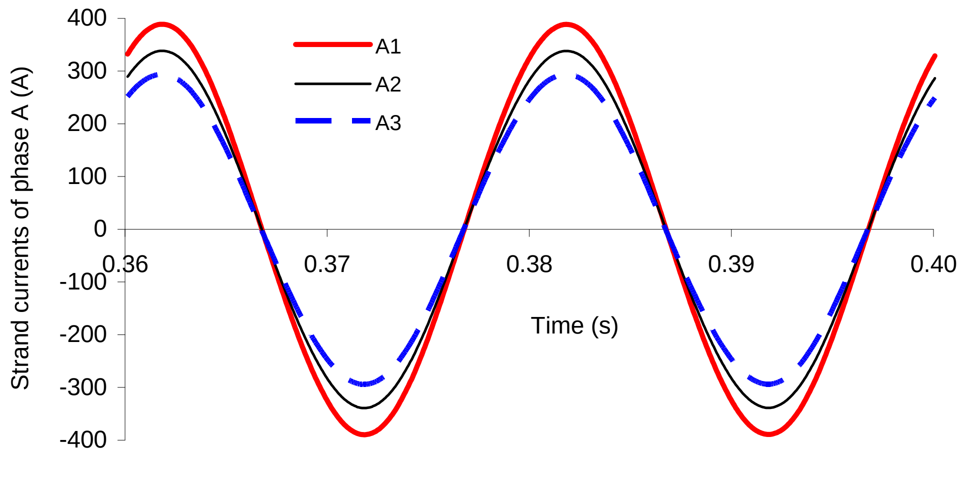

Figure 7: The strand-current variation of "phase A" with time for the non-transposed stator winding. The motor is supplied from a sinusoidal voltage source.

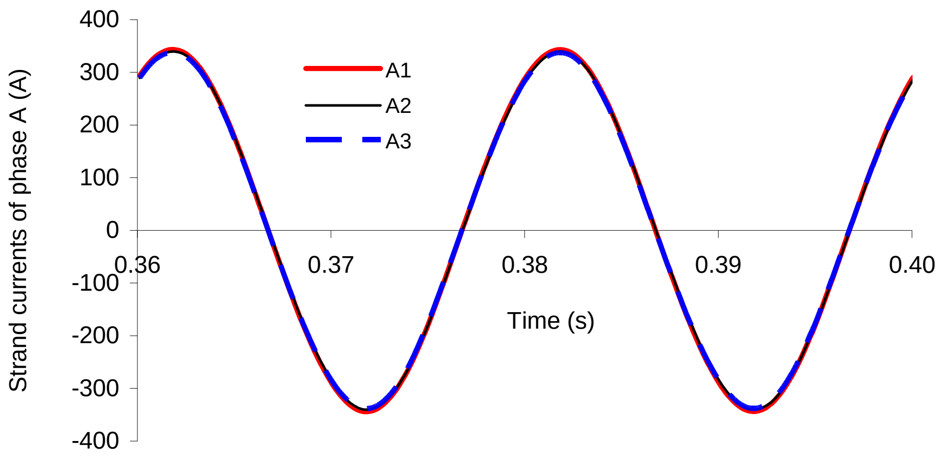

Figure 8: The strand-current variation of "phase A" with time for the transposed stator winding. The motor is supplied from a sinusoidal voltage source.

4.1.5 Optimum PWM supply for the motor at light load

An induction motor is designed to maintain high efficiency when it runs in the region over 75% of the rated load (Benbouzid et al. 1997, Xue et al. 2006). When the requirement of the load is changed to a light load, the efficiency of the motor becomes lower. With a changing load, control of the voltage is a possible technique to improve the efficiency (Lipo 1971, Jian et al. 1983). At no-load or a light load, a significant amount of losses can be reduced (Mohan 1980, Asghar & Ashfaq 2003). The study is performed for an inverter-fed motor. Control algorithms are used in commercial electric drives that optimise the losses by minimising the stator current based on an analytical motor model. To include the eddy-current losses in the optimisation, a more comprehensive loss model would be needed. As a first attempt, the fundamental harmonic voltage at the terminal is reduced from its rated voltage (690 V) by keeping the DC-link voltage constant (975 V). The modulation is changed by changing the flux-weakening frequency (Islam & Arkkio 2008b) of the PWM supply. The slip is adjusted to reach a particular load while changing the fundamental harmonic terminal voltage. The stator resistive loss remains almost the same and there is very little scope for the reduction of the total resistive loss (Publication P4).

Next, the fundamental harmonic terminal voltage is reduced from its rated voltage by reducing the DC-link voltage for the same modulation at the rated load. The reduction of the stator resistive losses is presented in Figure 9 as a function of the fundamental harmonic terminal voltage for 25%, 50%, and 75% of the rated load. The reduction of the losses is calculated by comparing the losses at the rated voltage (690 V). The total electromagnetic loss of the motor can be reduced significantly by changing the DC-link voltage together with the fundamental harmonic terminal voltage. The result presented here is the conclusive result of publication P4.

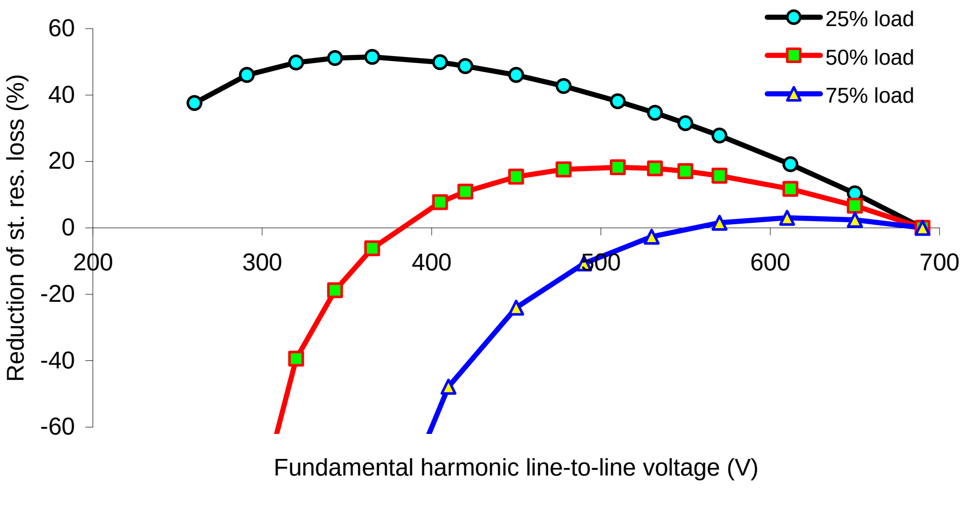

Figure 9: The reduction of stator resistive losses in percent compared to the losses at the rated voltage (690 V) presented as a function of the fundamental line-to-line voltage. The study is carried out for 25%, 50%, and 75% of the rated load for the PWM supply.

4.1.6 Accuracy of the finite-element discretisation

To compute the eddy-current loss in the stator winding accurately, finite-element discretisation is an important issue. The stator bars must be discretised with a detailed enough mesh. To study the accuracy of the finite-element discretisation, the number of elements per bar is increased by making more subdivisions over the bar height and width. On the basis of the number of finite-element layers, the discretisation in the direction of the bar height can be divided into three cases. Figure 10 presents the finite-element discretisation for all the three cases.

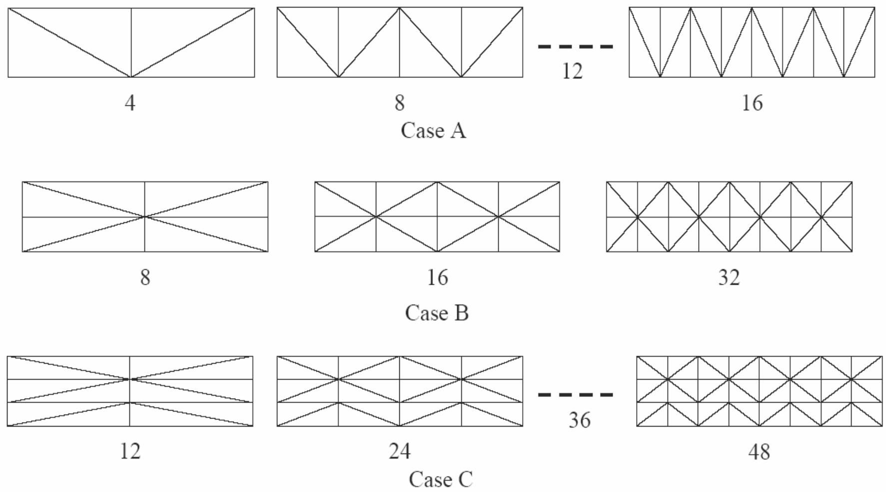

Figure 10: Finite-element discretisation of a bar in stator winding.

For case A, there is only one layer over the height. In a similar way, making a two- and three-layer finite-element discretisation over the bar height leads to case B and C. For each case, the number of finite elements is increased by making more subdivisions in the bar width. Figure 11 presents the dependency of the eddy-current loss of the stator winding on the finite-element discretisation as a function of the number of finite elements in a stator bar. The eddy-current losses are presented for the sinusoidal supply in Figure 11a and for the PWM supply in Figure 11b.

The results are computed when the motor is at the rated load and the distance from the inner surface of the stator to top of the stator bars, h_{sb}, is equal to 7.8 mm. The number of rotor slots is adjusted from 86 to 84 to reduce the symmetry sector. This adjustment increases the eddy-current losses about 0.2 kW since the slot harmonics are different. This is considered as a harmless modification when the objective is to compare the effects of the different finite-element discretisations.

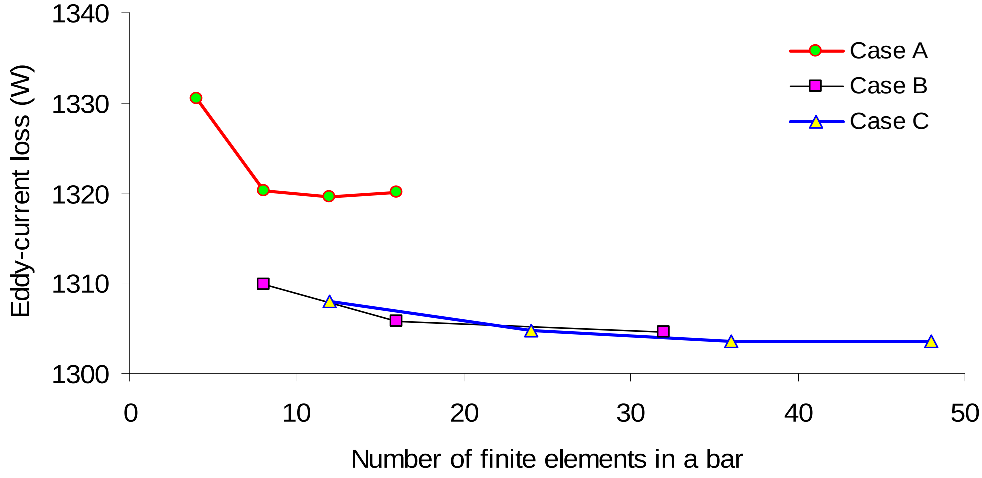

a)

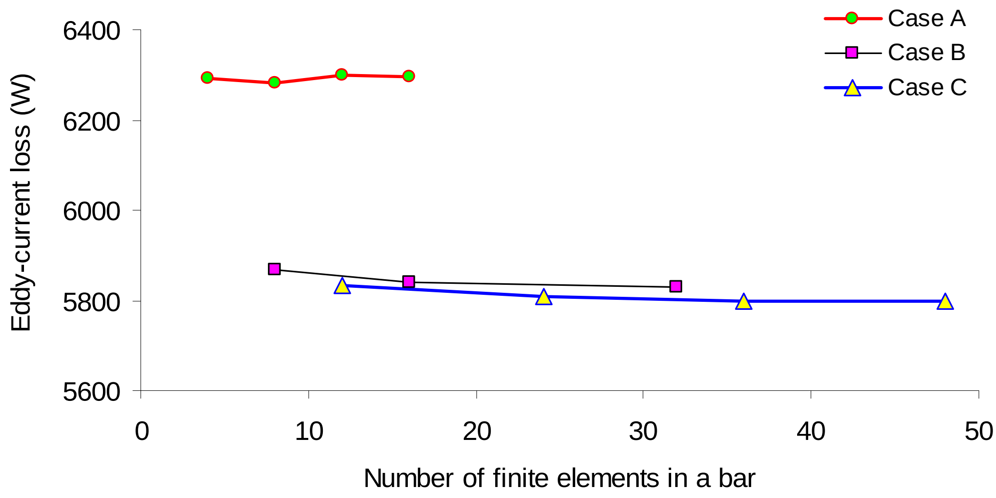

b)

Figure 11: Eddy-current loss as a function of the number of finite elements in a bar for: a) a sinusoidal and, b) a PWM supply. The study is carried out at the rated load.

The accuracy of the eddy-current loss calculations is improved by increasing the number of finite elements. For the sinusoidal supply, the maximum improvement is 2.0% of the eddy-current loss of the stator winding. This is only 0.28% of the total stator resistive loss. By moving from a single layer to double layer, the accuracy is increased already 0.21% of the stator resistive loss. For the PWM supply, by moving from a single layer to a double layer, the accuracy is improved by 6.7% of the eddy-current loss, which is 2.8% of the stator resistive loss. So the single-layer finite-element discretisation does not provide an accurate enough solution. In cases B and C, by increasing the number of finite elements, the improvement in accuracy is very small. For both the supplies, case B, in which the number of finite elements is 8 (Fig. 2b), provide a compromise, regarding the computational complexity and accuracy. For the sinusoidal supply, case A, in which the number of finite elements is 4 (Fig. 2a), can also be used with a considerable accuracy. More details can be found in publication P5.

4.2 Doubly-fed induction generator

4.2.1 Simulated machine

A 1.7-MW doubly-fed induction generator (DFIG), which has a 3-phase, 50-Hz, 690-V, delta-connected stator winding and a 3-phase, star-connected rotor winding, is considered. The data of the generator are presented in Table 2.

Table 2: Data of the machine that was studied.

Number of pole pairs	2
Number of stator parallel branches	4
Number of rotor parallel branches	1
Number of parallel strands in a stator coil	1
Number of parallel strands in a rotor coil	1
Number of stator slots	48
Number of rotor slots	60
Number of teeth in a stator coil pitch	10
Number of teeth in a rotor coil pitch	15
Inner diameter of the stator core (mm)	515
Outer diameter of the rotor core (mm)	509
Effective length of the machine (mm)	780
Rated slip (%)	–10

There are 10 effective turns in a stator slot and only one strand in a stator phase, which means there are 10 bars per slot. For a double-layer winding, every coil side consists of 5 effective turns. A rotor phase contains only one strand. There are 4 effective turns in a rotor slot, which means 4 bars per slot. The dimensions of the rotor slot are presented in Figure 12a and those of the stator slot in Figure 12b.

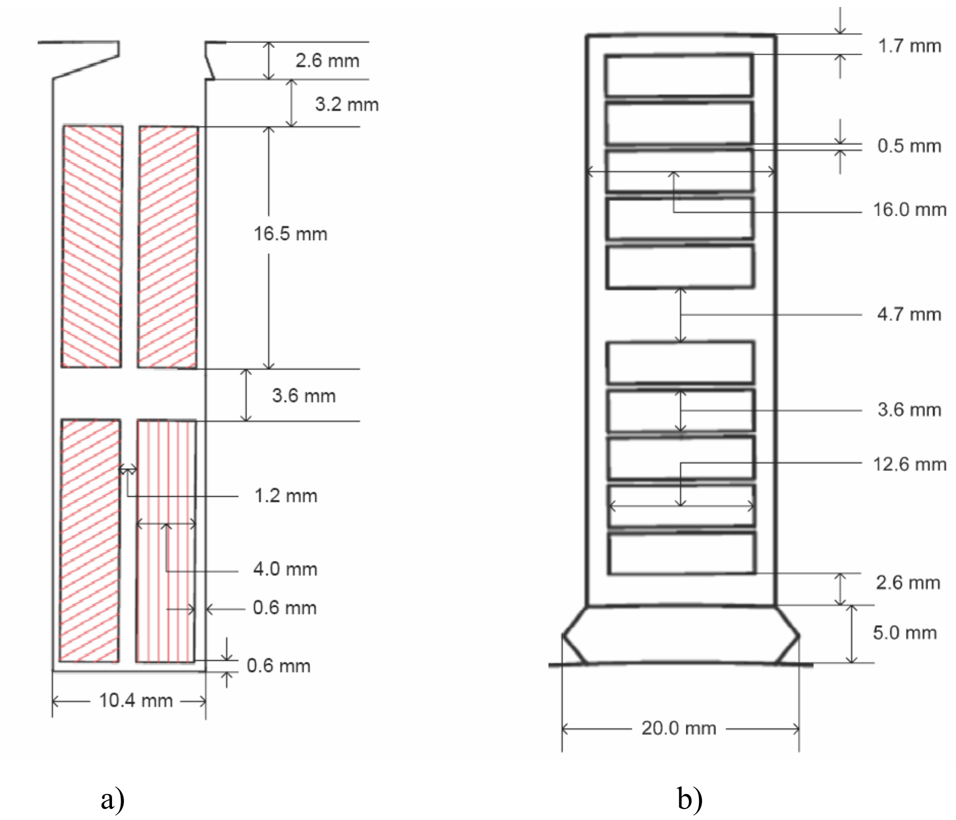

Figure 12: Dimensions of a) rotor slot, b) stator slot for the 1.7-MW DFIG.

The rated frequency of the rotor, i.e. the slip frequency, is –5 Hz since the rated slip of the generator is –10%. The rotation speed changes with the wind speed. The speed range of operation for the generator is from 1350 to 1950 rpm. The variation of slip within this generator speed range is from +10% to –30%. The slip range +10% to –10% belongs to the power optimisation region. In this region, the output energy is mainly optimised by adjusting the turbine speed as a function of wind speed (Hansen et al. 2003).

The output power varies in a manner approximately proportional to the third power of the generator speed (Miller 1997, Tapia et al. 2003). From –10% to –30% is the power limitation region, where the output power is limited to its rated value (Nunes et al. 2004, Seman et al. 2006a, Seman 2006). A second-order isoparametric finite-element discretisation is used to simulate the electrical machine. Using the symmetry, only a quarter of the electrical machine is solved with the finite-element solver. The flux density distribution of the generator is presented in Figure 13 using magnetic equipotential lines at the rated load. The time-discretised FEM model required 3 hours of CPU time to simulate a 0.6-second transient time using a 0.05-ms time-step size. There were 12 515 nodes in the FE model. A Pentium 4, dual core 2.6 GHz computer was used for the simulation. The Newton-Raphson method typically converged in 3-5 iterations.

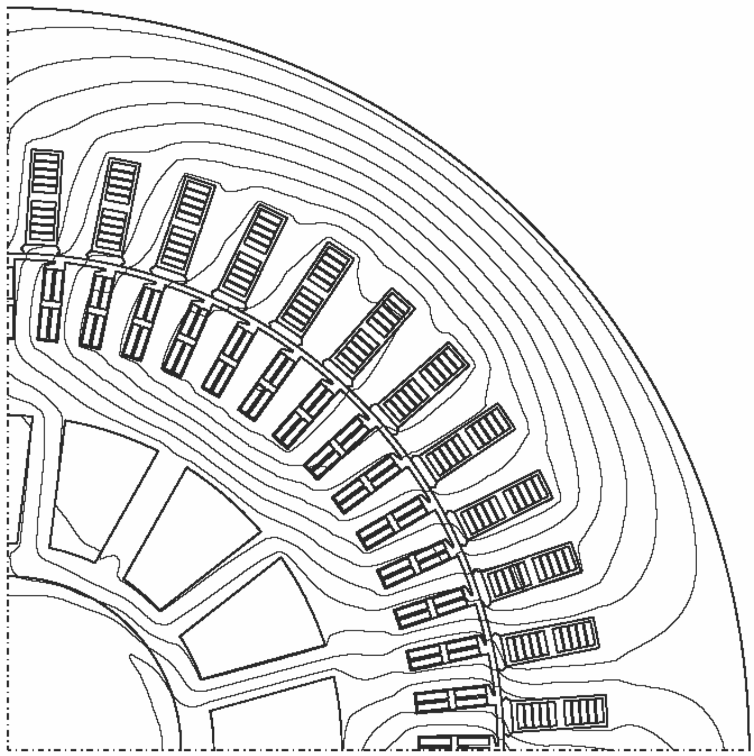

Figure 13: The flux-density distribution is presented using magnetic equipotential lines.

4.2.2 Effects of the rotor supply

Even though the DFIG is supplied from a static frequency converter to the rotor phases (Iov et al. 2003, Ledesma and Usaola 2005), the rotor of the generator is supplied from a sinusoidal voltage source to get reference data for the frequency converter supply. The stator voltage is sinusoidal as it is directly connected to the grid via a main transformer (Kanerva et al. 2005, Seman et al. 2006b).

The DFIG is controlled by supplying the rotor winding from a back-to-back frequency converter (Seman et al. 2006c). This connection brings a lower inverter cost, improves the efficiency, and allows the power factor of the wind turbine system to be controlled accurately (Müller et al. 2002). Most DFIG wind-turbine systems use a constant DC-link voltage (Arnalte et al. 2002, Nunes et al. 2004, Seman 2006) in the rated operating range. In the simulation, the rotor is supplied from a pulse-width-modulated (PWM) voltage source. For different rotor speeds, different fundamental harmonic (FH) voltages are obtained from a constant DC-link voltage (975 V) by changing the modulation (Islam and

Arkkio 2008b). The eddy-current effects ($k_{\text{eddy}} - 1$) of the rotor winding as a function of the generator speed are presented in Figure 14 and those of the stator winding in Figure 15 for both the sinusoidal and PWM supplies of the rotor. The operation points for different speeds are obtained by adjusting the input parameters manually based on the results of the time-harmonic analysis. This creates some hazy variation in the results of the time-discretised analysis.

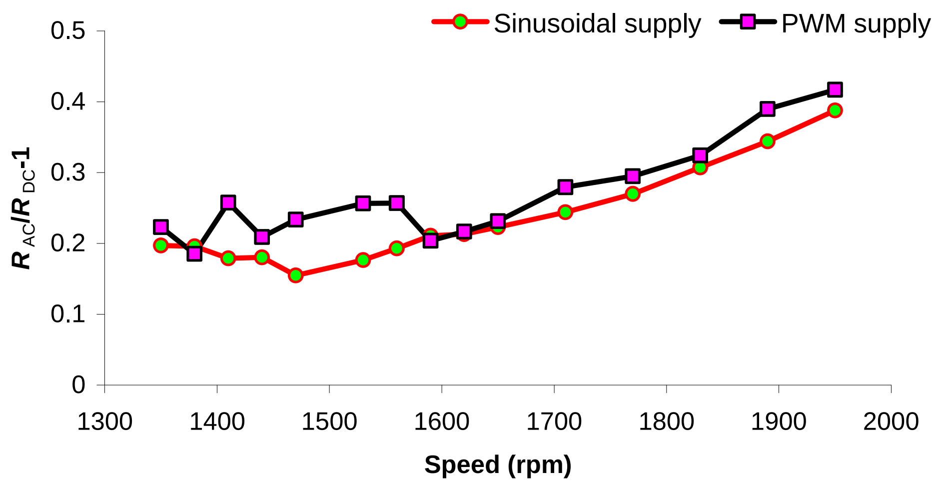

Figure 14: Eddy-current effects $(k_{\text{eddy}} - 1)$ of the rotor winding are presented as a function of speed when the rotor of the DFIG is supplied from a sinusoidal or PWM voltage source. The shaft powers and torques of the simulation points are shown in Figure 16.

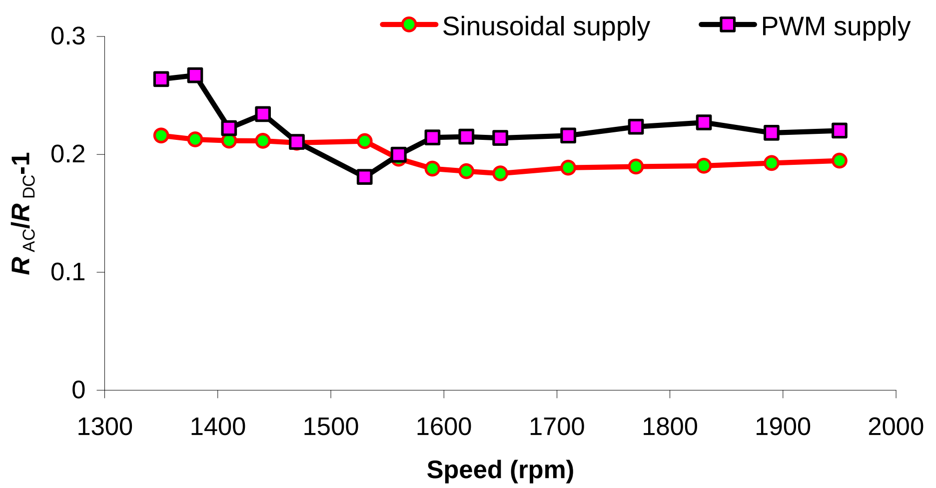

Figure 15: Eddy-current effects $(k_{\text{eddy}} - 1)$ of the stator winding are presented as a function of speed when the rotor of the DFIG is supplied from a sinusoidal or PWM voltage source. The shaft powers and torques of the simulation points are shown in Figure 16.

The additional eddy-current loss in the rotor of the DFIG resulting from the PWM supply is small compared to the resistive rotor loss of the sinusoidal supply. To compare the results, the fundamental harmonic of the rotor terminal voltage is kept equal to the sinusoidal supply for a particular speed. The shaft power and air-gap torque are presented in Figure 16, both for the PWM and sinusoidal supplies of the rotor as a function of generator speed.

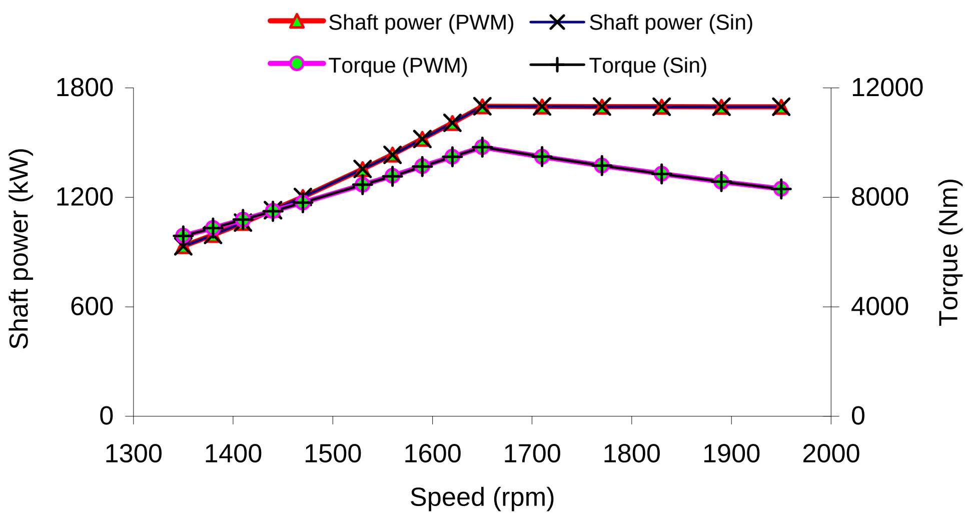

Figure 16: The shaft power and air-gap torque are presented as a function of rotational speed, both for the PWM and sinusoidal supplies of the rotor.

4.3 Verification

4.3.1 Comparison with an analytical model

To verify the time-harmonic and time-discretised eddy-current models, the eddy factor calculated for the 1250-kW cage induction motor (Table 1) is compared with the results from the analytical calculations. The motor is supplied from a sinusoidal voltage source. The number of finite elements per bar is 4 (Figure 2a) for the finite element simulations. In the analytical formulation, the conductor was modelled using Maxwell's equations assuming that flux in the slots is one-dimensional. More details can be found in Lammeraner et al. (1966) and Vogt (1983). According to the assumptions of the analytical model, the following conditions are applied during the calculations in the finite-element models:

1. The relative permeability of the core and shaft is very large and constant (10^9).
2. The stator windings are totally transposed, meaning there are no circulating currents in the parallel windings.

3. The conductors in the slot are lifted high enough (h_{sb} equal to 27.8 mm) for the effects of the radial main flux to be neglected.
4. The motor is at the blocked rotor condition, meaning that there are no higher harmonics resulting from the stator and rotor slottings or movement of the rotor.

Figure 17 presents the eddy factor variation for the analytical, time-harmonic and time-stepping methods as a function of frequency. Figure 18 presents the difference in the analytical eddy factor in relative value as a function of frequency. The frequency is varied from 10 Hz to 1000 Hz.

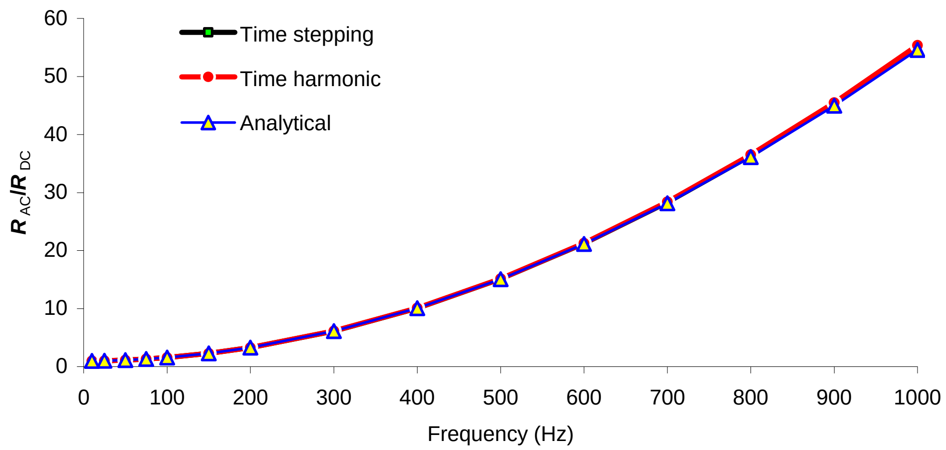

Figure 17: Verification of the developed numerical methods with an analytical one. Eddy factors are presented as a function frequency.

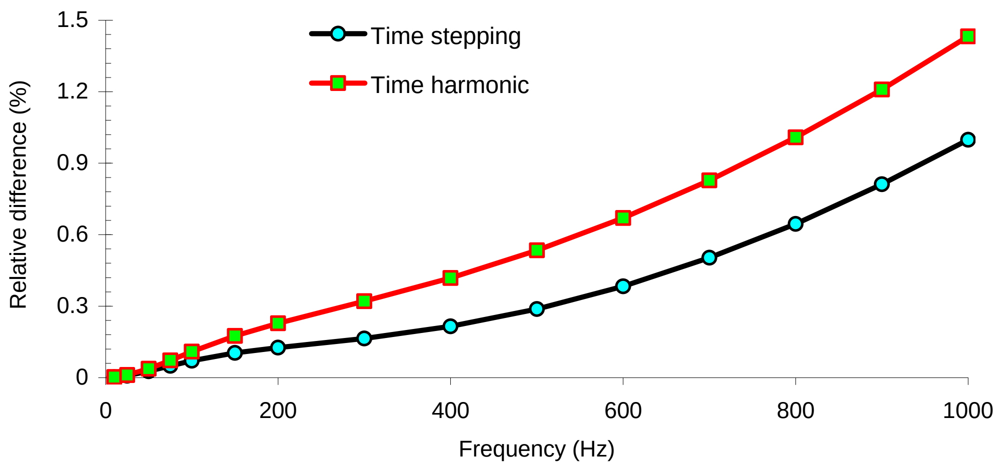

Figure 18: The percentage of the relative difference to the analytical eddy factors presented as a function of frequency.

The results of the time-harmonic and time-discretised finite-element methods agree well with the results of the analytical calculation. At the rated frequency, the relative difference is only 0.027%. The relative difference increases with an increase in frequency but even at 1000 Hz, the difference is only 1.43% for the time-harmonic and 1.0% for the time-discretised finite-element methods.

4.3.2 Power balance

After consideration of the eddy currents in the windings, the power balance is studied to justify the finite-element analysis (FEA). The small relative errors in power balance justify that the eddy-current model works properly and is compatible with the other formulations used for the FE model. The torque is calculated according to the equation for finite-element analysis derived by Coulomb (1983). The shaft power is calculated from the torque and rotational speed of the machine. In the FEA, the iron core is modelled as a non-conducting and non-linear material having a single valued magnetisation curve. An estimate for the iron losses is obtained as post-processing using empirical models (Arkkio 1987, Belahcen & Arkkio 2008) based on the Steinmetz formula. As a result, the core losses are not included in the power balance.

Cage induction motor

The power balance of the cage induction generator is studied after considering the eddy currents in the stator winding. The results from the power balance of the time-discretised FEA are presented in Table 3. These results are calculated when the motor is supplied from a sinusoidal voltage source. The relative error is calculated as a percentage of the input power.

Table 3. Power balance of the cage induction motor (CIM).

	No-load	Rated load	Locked-rotor
Input power (kW)	6.264	1209.92	1318.29
Stator resistive loss (kW)	1.799	9.59	414.48
Rotor resistive loss (kW)	1.272	6.29	909.28
Shaft power (Coulomb's method) (kW)	3.170	1194.41	00.00
Relative error (%)	0.367	0.031	0.415

The agreement of the power balance of the cage induction motor after the inclusion of the eddy currents in the stator winding is very good. At the rated load, the relative error is only 0.031%. At no-load, the relative error is 0.367% and at the locked-rotor condition it is 0.415%.

Doubly-fed induction generator

The power balance of the DFIG is considered for justification after consideration of the eddy currents both in the stator and rotor windings. The power balance of the time-discretised FEA is presented in Table 4. These results are calculated when both the stator and rotor supply are sinusoidal.

Table 4. Power balance of the doubly-fed induction generator (DFIG).

	No-load	Rated load	Locked-rotor
Input power to the stator (kW)	–11.815	–1529.93	1621.012
Power fed through slip rings (kW)	0.000	–131.24	0.003
Stator resistive loss (kW)	2.074	13.23	570.043
Rotor resistive loss (kW)	0.476	25.16	1051.160
Shaft power (Coulomb's method) (kW)	–14.350	–1700.01	00.00
Relative error (%)	0.127	0.029	0.012

The agreement of the power balance of the doubly-fed induction generator after the inclusion of the eddy currents both in the stator and rotor winding is very good. At the rated load, the relative error is only 0.029%. At no-load, the relative error is 0.127% and at the locked-rotor condition it is 0.012%.

5 Discussion

The scientific contributions of the dissertation listed in Section 1.3 are discussed one by one in Section 5.1. The discussion is started with a short summary of the contribution made by the work in every first paragraph and its significance in every second paragraph. Section 5.2 discusses the drawbacks of the methods that were developed and Section 5.3 contains proposals for future work.

5.1 Summary and significance

The time-harmonic finite-element method was developed to model eddy currents in the form-wound multi-conductor windings of electrical machines. The series and parallel connected bars were taken into account in the field and circuit equations. The equations were solved together as a strongly coupled system. The model was applied to the stator winding of a cage induction motor and the stator and rotor winding of a doubly-fed induction generator (DFIG). The model was also used to study the circulating currents between the parallel paths of the electrical machines.

The time-harmonic method was mainly developed to compute the initial values for time-discretised FEM. Such a numerical tool has not been found in the literature. Even though the time-harmonic model is computationally efficient, it cannot consider the higher harmonics resulting from the stator and rotor slots, the rotation of the rotor, and saturation. The time-harmonic model gives quite reliable current versus speed behaviour for both CIM and DFIG. However, the problems in modelling harmonic fields can be clearly seen when predicting the torque versus speed behaviour of CIM. Machine designers should be careful if they use only this tool for design purposes when considering eddy currents. The tool can be used reliably to study the currents circulating between the parallel paths of the electrical machine.

A time-discretised FEM was developed to consider eddy and circulating currents in the form-wound multi-conductor windings of electrical machines. Similarly to the time-harmonic model, the series and parallel connected bars were taken into account in the field and circuit equations. The equations were solved together as a strongly coupled system at every time step. The Backward Euler method was used for the time discretisation. The method was used for the stator winding of a cage induction motor and for the stator and rotor winding of a DFIG. The effects of eddy currents resulting from the higher harmonics generated by the stator and rotor slottings and the rotation of the rotor were studied. To study the effects, the results obtained from the time-discretised FEM model were compared with the results obtained from the time-harmonic FEM.

The time-discretised FEM that was developed provides a more comprehensive numerical tool to study the electromagnetic field and losses considering eddy currents and circulating currents in the series and parallel connected windings. In the literature, a time-discretised FEM model was also found to consider eddy currents in the multi-conductor windings of an electrical machine (Yatchev et al. 1995). Their model considered series-connected bars only and was not used to model the currents circulating in the parallel bars. Later on, Szücs (2001) used that model (Yatchev et al. 1995) and implemented macro-elements in the finite-element analysis for the stator winding of a cage induction motor. The main focus of his work was to study the savings of computation time and memory by using macro-elements. Studying the eddy-current effects both in the stator and rotor winding of a DFIG by solving the system of equations as strongly coupled includes some novelty. The time-discretised FEM model can take proper consideration of the higher harmonics that are generated from the stator and rotor slots, the rotation of the rotor, and magnetic nonlinearity. The developed numerical method can be used as a tool to design a more efficient and reliable electrical machine by studying the eddy currents properly.

The time-discretised finite-element method was used to study the eddy-current effects in form-wound stator windings caused by a non-sinusoidal supply. A pulse-width-modulated (PWM) voltage supply was used to supply the stator in the simulation of the cage induction motor. The PWM supply was obtained by using sinus-triangle comparison. To study the effect of the PWM supply on the eddy currents, the motor was first supplied from a PWM voltage source and then from a sinusoidal voltage source with an equal fundamental harmonic. The additional eddy-current loss in the stator winding of the motor was rather large because of the PWM supply.

In the literature, it can be found from the measurement of the total losses (Arkkio 1991, Joksimović & Binder 2003) or from the temperature rise test (Fouladgar & Chauveau 2005) that the non-sinusoidal supply increases the eddy-current losses in induction motors. However, there has not hitherto been a comprehensive numerical tool to consider the eddy currents in the winding for studying these effects properly. If a motor is used for a variable-speed application, the machine designer should be aware of it early in the design process, especially because of the eddy currents in the winding. It is possible to design a more efficient and reliable machine for a particular frequency converter supply. The optimum supply can be obtained for the particular machine by making simulations and analysing the results.

Time-discretised FEM was used to study the effect of the frequency-converter supply on the eddy currents in the form-wound rotor winding of a doubly-fed induction generator (DFIG). A similar PWM voltage source to that used to supply the stator of the cage induction motor was used to supply the rotor of the DFIG. To estimate the effect of the frequency converter on the eddy-current loss, a sinusoidal supply with an equal fundamental harmonic was also used to supply the rotor.

The additional eddy-current loss produced by the frequency converter in the rotor of the DFIG compared to the sinusoidal supply was very small (Publication P6). A cage induction motor with 3.2-mm-high copper conductors produced a significant additional eddy-current loss in the stator winding when supplied from a PWM voltage source with a 2-kHz switching frequency and 975-V DC-link voltages (Publication P3). With the same switching frequency and DC-link voltage, and much higher (16.5-mm) copper conductors, the additional eddy-current loss in the rotor winding of the DFIG was negligible. Because of the large inductances of the rotor winding compared to the ones of the stator, much higher conductors can be used in the rotor winding of a DFIG than in the stator winding of an inverter-fed cage induction motor.

The effect of the radial distance from the inner surface of the stator to the position of the first stator bar (h_{sb}) on eddy currents was studied. The study was carried out using the time-harmonic and time-discretised finite-element methods. Both the sinusoidal and PWM voltage supplies were used to study this parameter using time-discretised FEM. The study was performed by placing the coils very close to the air gap and gradually increasing the distance. The parameter (h_{sb}) was found to be a very important design parameter. The consequences would be dangerous if the coils were very close to the air gap.

The importance of the position of the coil has been understood earlier (Richter 1951, Oberretl 1969). Different kinds of simple analytical methods to study the eddy current effects for a given main flux can be found in Richter (1951). Oberretl (1969) gave thirteen rules to minimise the stray load losses in induction motors. Rule number seven described the position of the stator coil in a stator slot by clarifying its relationship to the slot width. For an open stator slot, the ratio between the width of the slot and the height from the inner surface of the stator to the top of the stator coils must be less than or equal to three. To keep the ratio equal to or less than one is not economical or practical when building a machine. An acceptable value for distance, h_{sb}, can be studied both from the loss and thermal points of view. If a 10% increase in the resistive losses is allowed related to the h_{sb} variation, the minimum distance of the stator coil from the air gap is about 6 mm. The IEC 60034-1 (2004) standard specifies for motors within the power range 200–5000 kW that the highest average temperature allowed for a class 155 insulation is 145 °C. The maximum temperature within the insulation can be 155 °C. This gives a 10 degrees difference between the maximum and average temperatures. It can be seen from Figure 5 that the 10 degree temperature difference is reached at a h_{sb} value of 6 mm. Both the loss and thermal points of view lead to the 6 mm minimum distance. The rule given by Oberretl (1969) seems to be defined for too wide a range.

The circulating currents in the parallel stator conductors were modelled using both time-harmonic and time-discretised FEM. The effect of circulating currents was studied for the form-wound multi-conductor winding of a cage induction motor. A transposition technique was also developed by modifying the connection matrix between the bars and parallel strands. The systematic transposition of the stator winding reduced the circulating currents between the parallel strands to practically zero.

Studies of circulating currents in form-wound windings based on 2-D FEM analysis were not found in the literature. The circulating currents seem to be mainly induced by the fundamental flux. Therefore, the time-harmonic model gives a reliable estimation to study the circulating currents. The method that was developed can also be used to study the circulating currents of random-wound windings of electrical machinery. However, the problem size may become too high to study the circulating currents for a practical random-wound winding machine.

5.2 Drawbacks of the methods

The drawbacks of the methods that were developed are listed below:

- The developed methods are so-called brute force methods. The methods require the detailed finite-element discretisation of the problem region for proper modelling. The requirements of computation time and memory are increased with an increasing number of bars or conductors. If there is a very high number of series and parallel connected conductors, it might be impossible to model the phenomena. The homogenisation technique or macro elements could be used to study for a large number of conductors.
- The methods need very detailed data regarding the winding construction of the machine. It may be difficult to get these data because of the confidentially matters.
- The iron core was modelled as non-conducting and non-linear material with a single value magnetisation curve. The iron losses were obtained as post-processing and were not included in the field equation. Dlala (2008) has developed a magneto-dynamic vector hysteresis model for the steel laminations of rotating electrical machines. The model could be combined with the eddy-current methods that were developed to obtain a more comprehensive numerical method. The accuracy, efficiency, stability, advantages and disadvantages of the different finite-element formulations related to core-loss modelling have been investigated by Dlala (2009).

5.3 Future work

Several applications related to eddy currents in the windings of electrical machines were studied using the time-harmonic and time-discretised finite-element circuit models developed here. Using these methods, it would be possible to study even more phenomena with comparatively little effort. These tasks are listed below as future work:

- The method can be applied to different kinds of electrical machines to obtain general rules for the placement of the coils in the slot of the machine.
- Search for an optimal height and width of the bars by changing the number of parallel strands and by reorganising the bars, as well as the strands, of the coils.
- Search for an optimal height and width of the stator slots by changing the bar height.

- Study a high-speed machine, in which random-wound winding is more common. Studying the randomisation by considering both the eddy currents and circulating currents would be interesting.
- Search for an optimal transposition of stator winding for electrical machines for which systematic and perfect transposition is not possible.
- Study different kinds of non-sinusoidal supplies to find an optimum supply.
- This method can be used to identify a simple stator loss model for the control algorithm used in frequency converters.

6 Conclusions

Time-harmonic and time-discretised finite-element circuit models were developed to calculate the eddy currents in the form-wound multi-conductor windings of electrical machines. The methods were applied to the stator winding of a 1250-kW cage induction motor and to both the stator and rotor windings of a 1.7-MW doubly-fed induction generator (DFIG). The bars connected in series and parallel were discretised and identified in the mesh generator program. In time-harmonic FEM, the system of equations was solved with the Newton-Raphson iteration method for the steady-state solution. In time-discretised FEM, the Newton-Raphson iteration method was used to solve the system of equation at every time step. The time-discretisation was performed using the Backward Euler method.

The radial distance from the inner surface of the stator to the top of the stator winding was found to be an important design parameter. The severity of this parameter was presented by performing a simulation with finite-element eddy-current models. The circulating currents were also modelled in the parallel stator conductors of a cage induction motor. A transposition of the conductors was implemented to reduce the circulating currents. The eddy-current effects in the form-wound multi-conductor stator winding of the cage induction motor with a non-sinusoidal supply were studied. A pulse-width-modulated (PWM) voltage supply was achieved by sinus triangle comparison and used to supply the motor. A PWM supply produces a significant amount of additional eddy-current losses in the form-wound stator winding of the cage induction motor, compared to the sinusoidal supply. Sinusoidal and PWM supplies with an equal fundamental harmonic were used for two different simulations to compare the results. Similar sinusoidal and PWM voltages were used to supply the rotor winding of the DFIG as well. The additional eddy current losses in the form-wound rotor winding resulting from the PWM supply are small compared to the sinusoidal supply.

References

Arkkio, A. 1987: “Analysis of induction motors based on the numerical solution of the magnetic field and circuit equations”, *Acta Polytechnica Scandinavica, Electrical Engineering series* No. 59. Helsinki, Finland. (1987) 97 p. Available: http://lib.tkk.fi/Diss/198X/isbn951226076X/

Arkkio, A. 1990: “Finite element analysis of cage induction motors fed by static frequency converters”, *IEEE Transaction on Magnetics* Volume 26, Issue 2, March 1990, pp. 551–554.

Arkkio, A. 1991: “Analysis of a 37 kW cage-induction motor”, *Laboratory of Electromechanics, Helsinki University of Technology,* Report 30, Finland, 1991, 64 p.

Arnalte, S.; Burgos, J. C.; Rodríguez-Amenedo, J. L. 2002: “Direct torque control of a doubly-fed induction generator for variable speed wind turbines”, *Electric Power Components and Systems,* Volume 30, 2002, pp. 199–216.

Asghar, M. S. J.; Ashfaq, H. 2003: “Speed control of wound rotor induction motors by AC regulator based optimum voltage control”, *IEEE Conference Record of the 5th International Conference on Power Electronics and Drive Systems*, Volume 2, 17-20 November 2003, pp. 1037–1040.

Ausserhofer, S.; Biro, O.; Preis, K. 2007a: “An efficient harmonic balance method for nonlinear eddy-current problems” *IEEE Transactions on Magnetics*, Volume 43, Issue 4, April 2007, pp. 1229–1232.

Ausserhofer, S.; Biro, O.; Preis, K. 2007b: “Frequency and time domain analysis of nonlinear periodic electromagnetic problems”, *International Conference on Electromagnetics in Advanced Applications*, 17 – 21 September 2007, pp. 229–232.

Bastos, A.; Sadowski N. 2003: “Electromagnetic modeling by finite element methods”, Marcel Dekker, Inc. New York. Basel. ISBN 0-8247–4269-9.

Baodong, B.; Dexin, X.; Jiefan, C.; Zhenyao, F; Mohammed, O. A. 1995: “Optimal transposition design of transformer windings by genetic algorithm”, *IEEE Transactions on Magnetics*, Volume 31, November 1995, pp. 3572–3574.

Belahcen, A.; Arkkio, A. 2008: “Comprehensive dynamic loss-model of electrical steel applied to FE simulation of electrical machines”, *IEEE Transaction on Magnetics,* Volume 44, Issue 6, June 2008, pp. 886–889.

Benbouzid, M. E. H.; Beguenane, R.; Dessoude, M.; Hubbi, W. 1997: “Energy optimize control strategy for a variable input voltage three-phase induction motor”, *IEEE International Electric Machines and Drives Conference Record*, 18 – 21 May 1997, pp. MD2/5.1–MD2/5.3.

Bennington, B. J.; Breenner, W. C. 1970: “Transposition in turbogenerator coil sides short circuited at each end”, *IEEE Transactions on Power Apparatus and Systems*., Volume 89, Issue 8, November 1970, pp. 1915–1921.

Bíró, O.; Preis, K. 2006: “An efficient time domain method for nonlinear periodic eddy current problems” *IEEE Transactions on Magnetics*, Volume 42, Issue 4, April 2006, pp. 695–698.

Boglietti, A.; Bottauscio, O.; Chiampi, M.; Pastorelli, M.; Repetto, M. 1996: “Computation and measurement of iron losses under PWM supply conditions”, *IEEE Transactions on Magnetics*, Volume 32, Issue 5, September 1996, pp. 4302–4304.

Carpenter, C. 1975: “A network approach to the numerical solution of eddy-current problems” *IEEE Transactions on Magnetics*, Volume 11, Issue 5, September 1975, pp. 1517–1522.

Chari, M. V. K.; Silvester, P. 1971a: “Analysis of turboalternator magnetic fields by finite elements”, *IEEE Transactions on Power Apparatus and Systems*, Volume 90, Issue 2, March 1971, pp. 454–464.

Chari, M. V. K.; Silvester, P. 1971: “Finite-element analysis of magnetically saturated D-C machines” *IEEE Transactions on Power Apparatus and Systems*, Volume 90, Issue 5, September 1971, pp. 2362–2372.

Chari, M. V. K.; Csendes, Z. J. 1977: “Finite element analysis of the skin effect in current carrying conductors”, *IEEE Transactions on Magnetics*, Volume 13, Issue 5, September 1977, pp. 1125-1127.

Chari, M. V. K.; Silvester, P. 1980: “Finite-elements in electrical and magnetic field problems” *John Wiley & Sons*, Chichester-New York-Brisbane-Toronto, 219 p.

Chari, M. V. K.; Bedrosian, G. 1982: “Electromagnetic field analysis of eddy current effects in rotating electrical apparatus and machinery”, *IEEE Transactions on Magnetics*, Volume 18, Issue 6, November 1982, pp. 1713–1715.

Ciric, I. R.; Hantila, F. I. 2007: “An efficient harmonic method for solving nonlinear time-periodic eddy-current problems”, *IEEE Transactions on Magnetics*, Volume 43, Issue 4, April 2007, pp. 1185–1188.

Coulomb, J. L. 1983: “A methodology for the determination of global electromechanical quantities from a finite element analysis and its application to the evaluation of magnetic forces, torques and stiffness”, *IEEE Transactions on Magnetics*, Volume 19, Issue 6, November 1983, pp. 2514–2519.

Dabrowski, M.; Demenko, A. 1988: “Hybrid method for analysis of eddy current loss in electrical machine winding caused by the main flux”, *IEEE Transactions on Magnetics*, Volume 24, Issue 1, January 1988, pp. 479–482.

Davat, B.; Ren, Z.; Lajoie-Mazenc, M. 1985: “The movement in the field modelling”, *IEEE Transactions on Magnetics*, Volume 21, Issue 6, November 1985, pp. 2296–2298.

Demenko, A. 2006: “Eddy Current Computation in 3-Dimensional Models for Electrical Machine Applications”, *Proceedings of the 12th Power Electronics and Motion Control Conference (EPE-PEMC)*, August 30 -September 1 2006, pp. 1931–1936.

Demerdash, N. A.; Hamilton, H. B.; Brown, G. W. 1972: “Simulation for design purposes of magnetic fields in turbogenerators with symmetrical and asymmetrical rotors Part I-Model development and solution technique”, *IEEE Transactions on Power Apparatus and Systems*, Volume 91, Issue 5, September 1972, pp. 1985–1992.

Demerdash, N. A.; Hamilton, H. B. 1972a: “Simulation for Design Purposes of Magnetic Fields in Turbogenerators with Asymmetrical and Symmetrical Rotors Part II Model Calibration and Applications”, *IEEE Transactions on Power Apparatus and Systems*, Volume 91, Issue 5, September 1972, pp. 1992–1999.

Demerdash, N. A.; Hamilton, H. B. 1972b: “Effect of Rotor Asymmetry on Field Forms and Eddy Current Losses in Stator Conductors Due to Radial Flux”, *IEEE Transactions on Power Apparatus and Systems*, Volume 91, Issue 5, September 1972, pp. 1999–2010.

Demerdash, N. A.; Garg, V. K.; Hamilton, H. B. 1975: “Effect of ventilating holes on radial flux and losses in stator slots of turbogenerators”, *IEEE Transactions on Power Apparatus and Systems*, Volume 94, Issue 4, Part 1, July 1975, pp. 1177–1182.

Demerdash, N. A.; Nehl, T. W. 1979: “An Evaluation of the Methods of Finite Elements and Finite Differences in the Solution of Nonlinear Electromagnetic Fields in Electrical Machines” *IEEE Transactions on Power Apparatus and Systems*, Volume 98, Issue 1, January 1979, pp.74–87.

Dexin, X.; Xiuke, Y.; Yingying, Y.; Baodong, B; Takahashi, N. 2000: “Circulating current computation and transposition design for large current winding of transformer with multi-section strategy and hybrid optimal method”, *IEEE Transactions on Magnetics*, Volume 36, Issue 4, July 2000, pp. 1014–1017.

Dlala, E. 2008: “Magnetodynamic vector hysteresis models for steel laminations of rotating electrical machines”, TKK Dissertation 111, Espoo 2008, 165 p. Available: http://lib.tkk.fi/Diss/2008/isbn9789512292776

Dlala, E. 2009: “Comparison of models for estimating core losses in electrical machines using the finite-element method”, *IEEE Transactions on Magnetics*, Volume 45, Issue 2, February 2009, pp. 716–725.

Dwight, H. B. 1945: “Electrical coils and conductors” New York McGraw-Hill Book Company, Inc. 351 p.

El Feddi, M.; Ren, Z.; Razek, A.; Bossavit, A. 1997: “Homogenization technique for Maxwell equations in periodic structures”, *IEEE Transactions on Magnetics*, Volume 33, Issue 2, Part 2, March 1997, pp. 1382–1385.

Field, A. B. 1905: “Eddy currents in large slot-wound conductors”, *Trans. Am. Inst. Elect. Engg. 1905*, Volume 24, pp. 761–788.

Fouladgar, J.; Chauveau, E 2005: “The influence of the harmonics on the temperature of electrical machines”, *IEEE Transactions on Magnetics*, Volume 41, Issue 5, May 2005, pp. 1644–1647.

Garg, V.; Weiss, J. 1986: “Finite element solution of transient eddy-current problems in multiply-excited magnetic systems”, *IEEE Transactions on Magnetics*, Volume 22, Issue 5, September 1986, pp.1257–1259.

Gilman, R. E. 1920: “Eddy current losses in armature conductors”, *Trans. AIEE*, Volume 39, June-July 1920, pp. 997–1056.

Grant, D. A.; Stevens, M.; Houldsworth, J. A. 1985: “The effect of word length on the harmonic content of microprocessor-based PWM wave form generators”, *IEEE Transactions on Industry Applications*, Volume 21, Issue 1, January/February 1985, pp. 218–225.

Gyselinck, J.; Dular, P. 2004: “A time-domain homogenization technique for laminated iron cores in 3-D finite-element models”, *IEEE Transactions on Magnetics*, Volume 40, Issue 2, Part 2, March 2004, pp. 856–859.

Gyselinck, J.; Dular, P. 2005: “Frequency-domain homogenization of bundles of wires in 2-D magnetodynamic FE calculations”, *IEEE Transactions on Magnetics*, Volume 41, Issue 5, May 2005, pp. 1416–1419.

Gyselinck, J.; Robert, F. 2005: “Frequency- and time-domain homogenization of windings in two-dimensional finite-element models”, *European Conference on Power Electronics and Applications*, 11-14 September 2005, 10p.

Gyselinck, J.; Sabariego, R. V.; Dular, P. 2007: “Time-Domain Homogenization of Windings in 2-D Finite Element Models” *IEEE Transactions on Magnetics*, Volume 43, Issue 4, April 2007, pp. 1297–1300.

Haldemann, J. 2004: “Transpositions in stator bars of large turbogenerators”, *IEEE Transactions on Energy Conversion*, Volume 19, Issue 3, September 2004, pp. 553–560.

Hansen, A. D.; Jauch, C.; Sørensen, P.; Iov, F.; Blaabjerg, F. 2003: “Dynamic wind turbine models in power system simulation tool”, *Risø-R-1400.* Pitney Bowses Management Services Denmark A/S, December 2003, Denmark. ISBN-87-550-3198-6.

Hilderbrand, E. N.; Roehrdanz, H. 2001: “Losses in three-phase induction machines fed by PWM converters”, *IEEE Transactions on Energy Conversion*, Volume 16, Issue 3, September 2001, pp. 228–233.

Holmes, D. G; Lipo, T. A. 2003: “Pulse width modulation for power converters principle and practice”, *IEEE Series on Power Engineering*, A John Wiley & Sons, inc., Publication, 2003, 724 p.

IEC 60034-1, 2004: International standard, Rotating electrical machines – Part1: Rating and performance, 137 p.

Iov, F.; Blaabjerg, F.; Hansen, A. D 2003: “Analysis of a variable-speed wind energy conversion scheme with doubly-fed induction generator”, *International Journal of Electronics*, Volume 90, Issue 11-12, November 2003, pp. 779–794.

Islam, M. J.; Arkkio, A. 2006: “Circulating currents in the parallel stator conductors of electrical machines”, *Cd proceedings of XVII International Conference on electrical machines*, Chania, Crete Island, Greece, September 2006, 6 p.

Islam, M. J.; Pippuri, J.; Perho, J.; Arkkio, A 2007: “Time-harmonic finite-element analysis of eddy currents in the form-wound stator winding of a cage induction motor”, *IET Electric Power Applications*, Volume 1, Issue 5, September 2007, pp. 839–846.

Islam, M. J.; Arkkio, A. 2008a: “Time-stepping finite-element analysis of eddy currents in the form-wound stator winding of a cage induction motor supplied from a sinusoidal voltage source”, *IET Electric Power Applications*, Volume 2, Issue 4 July 2008, pp. 256–265.

Islam, M. J.; Arkkio, A. 2008b: “Optimum supply for an inverter-fed cage induction motor at different load conditions”, *Nordic Workshop on Power and Industrial Electronics*, 9 – 11 June 2008, TKK, Finland. Available: http://lib.tkk.fi/Conf/2008/urn011711.pdf

Islam, M. J.; Arkkio, A. 2009a: “Effects of pulse-width-modulated supply voltage on eddy currents in the form-wound stator winding of a cage induction motor”, *IET Electric Power Applications*, Volume 3, Issue 1, January 2009, pp. 50–58.

Islam, M. J.; Arkkio, A. 2009b: “Finite-element analysis of eddy-currents in the form-wound multi-conductor windings of a doubly-fed induction generator”, *Report Series on Electromechanics,* Report 75, Helsinki University of Technology, Espoo 2009, 20 p.

Jian, T. W.; Schmitz, N. L.; Novotny, D. W. 1983: “Characteristic induction motor slip values for variable voltage part load performances optimization”, *IEEE Transactions on Power Apparatus and Systems*, Volume 102, Issue 1, January 1983, pp. 38–46.

Joksimović, G; Binder, A. 2004: “Additional no-load losses in inverter-fed high-speed cage induction motors”, *Electrical Engineering,* Volume 86, pp. 105–116.

Kanerva, S.; Seman, S.; Arkkio, A. 2005; “Inductance model for coupling finite element analysis with circuit Simulation”, *IEEE Transactions on Magnetics*, Volume 41, Issue 5, May 2005, pp. 1620–1623.

Kladas, A.; Razek, A. 1988a: “Eddy currents modelling in synchronous machines during starting accounting for the nature of damper end connections” *IEEE Transactions on Magnetics* , Volume 24, Issue 1, January 1988, pp 186–189.

Kladas, A.; Razek, A. 1988b: “Numerical calculation of eddy currents and losses in squirrel cage motors due to supply harmonics”, *Proceedings of International Conference on Electrical Machines*, Volume 2, 12 – 14 September 1988, Pisa, Italy, pp 65–69.

Konrad, A. 1981: “The numerical solution of steady-state skin effect problems-An integrodifferential approach” *IEEE Transactions on Magnetics*, Volume 17, Issue 1, January 1981, pp. 1148–1152.

Konrad, A. 1982: “Integrodifferential finite element formulation of two-dimensional steady-state skin effect problems”, *IEEE Transactions on Magnetics*, volume 18, Issue 1, January 1982, pp. 284–292.

Konrad, A.; Chari, M.; Csendes, Z. 1982: “New finite element techniques for skin effect problems”, *IEEE Transactions on Magnetics*, Volume 18, Issue 2, March 1982, pp. 450–455.

Konrad, A. 1985: “Eddy currents and modelling”, *IEEE Transactions on Magnetics*, Volume 21, Issue 5, September 1985, pp. 1805–1810.

Krawczyk, A. Tegopoulos, J. A. 1993: “Numerical modelling of eddy currents”, *Monographs in Electrical & Electronic Engineering 32*, Oxford Science Publications, 116 p.

Lammeraner, J.; Štafl, M. 1966: “Eddy currents”, London, Iliffe Books Ltd., 1966, 233 p.

Ledesma, P.; Usaola, J. 2005: “Doubly fed induction generator model for transient stability analysis”, *IEEE Transactions on Energy Conversion*, Volume 20, Issue 2, June 2005, pp. 388–397.

Lee, J. J.; Kim, Y. K.; Nam, H.; Ha, K. H.; Hong, J. P.; Hwang, D. H. 2004: “Loss distribution of three-phase induction motor fed by pulsewidth-modulated inverter”, *IEEE Transactions on Magnetics*, Volume 40, Issue 2, March 2004, pp. 762–765.

Lipo, T. A. 1971: “The analysis of induction motors with voltage control by symmetrically triggered thyristors”, *IEEE Transactions on Power Apparatus and Systems*, Volume 90, Issue 2, March 1971, pp. 515–525.

Long, L. J.; Hamilton, H. B. 1975: **“**Simplified approach to radial flux loss calculation in cylindrical rotor generators”, *IEEE Transactions on Power Apparatus and Systems*, Volume 94, Issue 5, Part 1, September 1975, pp. 1680–1688.

Lu, J.; Yamada, S.; Bessho, K. 1990: “Time-periodic magnetic field analysis with saturation and hysteresis characteristics by harmonic balance finite element method”, *IEEE Transactions on Magnetics*, Volume 26, Issue 2, March 1990, pp. 995–998.

Lu, J.; Yamada, S.; Bessho, K. 1991: “Harmonic balance finite element method taking account of external circuits and motion”, *IEEE Transactions on Magnetics*, Volume 27, Issue 5, September 1991, pp. 4024–4027.

Lähteenmäki, J. 2002: “Design and Voltage Supply of High Speed Machines”. *Acta Polytechnica Scandinavica, Electrical Engineering series No. 108.* Helsinki, Finland, 140 p. Available: http://lib.tkk.fi/Diss/2002/isbn951226224X/

McWhirter, J.; Duffin, R.; Brehm, P.; Oravec, J. 1979: **“**Computational methods for solving static field and eddy current problems via Fredholm integral equations”, *IEEE Transactions on Magnetics,* Volume 15, Issue 3, May 1979, pp. 1075–1084.

Meeker, D. 2009: “Finite Element Method Magnetics”, User Manual, Version 4.2, 5 February, 2009, 155 p.

Mohan, N. 1980: “Improvement in energy efficiency of Induction motors by means of voltage control”, *IEEE Transactions on Power Apparatus and Systems*, Volume 99, Issue 4, July 1980, pp. 1466–1471.

Meco-Gutiérrez, M. J.; Pérez-Hidalgo, F.; Vargras-Merino, F.; Heredia-Larrubia, J.R 2007: “Pulse width modulation technique with harmonic injection and frequency modulated carrier: formulation and application to an induction motor”, *IET Electric Power Applications*, Volume 1, Issue 5, September 2007, pp. 714–726.

Miller, A.; Muljadi, E.; Zinger, D. S. 1997: “A variable speed wind turbine power control”, *IEEE Transactions on Energy Conversion*, Volume 12, Issue 2, June 1997, pp. 181–186.

Moreau, O.; Popiel, L.; Pages, J. L. 1998: “Proximity losses computation with a 2D complex permeability modelling” *IEEE Transactions on Magnetics,* Volume 34, Issue 5, Part 1, September 1998, pp. 3616–3619.

Müller, S.; Deicke, M., De Doncker, R. W. 2002: “Doubly fed induction generator systems for wind turbines”, *IEEE Industry Applications Magazine*, Volume 8, Issue 3, May-June 2002, pp. 26–33.

Nunes, M. V. A.; Lopes, J. A. P.; Zurn, H. H.; Bezerra, U. H.; Almeida, R. G. 2004: “Influence of the variable-speed wind generators in transient stability margin of the conventional generators integrated in electrical grids”, *IEEE Transactions on Energy Conversion*, Volume 19, Issue 4, December 2004, pp. 692–701.

Oberretl, K. 1963: “Die Ermittlung von magnetischen Feldern, Wirbelströmen und Kräften in komplizierten Fällen durch simulation and Gittermodellen”, Archiv für Elektrotechnik, Bd. 48, pp. 297–313.

Oberretl, K. 1969: “13 Regeln für minimale Zusatzverluste in Induktionsmotoren”, Bulletin Oerlikon 389/390, 11p.

Oberretl, K. 1969: “Magnetic fields, eddy currents, and losses, taking the variable permeability into account”, *IEEE Transactions on Power Apparatus and Systems,* Volume 88, Issue 11, November 1969, pp. 1646–1657.

Oberretl, K. 2007: “Losses, torques and magnetic noise in induction motors with static converter supply, taking multiple armature reaction and slot openings into account”, *IET Electric Power Applications*, Volume 1, Issue 4, July 2007, pp. 517–531.

Patecki, A.; Stępień, S.; Szymański, G. 2004: “Power losses analysis in the windings of electromagnetic gear”, The International Journal for Computation and Mathematics in Electrical and Electronic Engineering, Volume 23, Issue 3, pp. 748–757.

Preis, K.; Stogner, H.; Richter, K. 1982: "Calculation of eddy current losses in air coils by finite element method", *IEEE Transactions on Magnetics*, Volume 18, Issue 6, November 1982, pp. 1064–1066.

Preis, K. 1983: "A contribution to eddy current calculations in plane and axisymmetric multiconductor systems", *IEEE Transactions on Magnetics*, Volume 19, Issue 6, November 1983, pp. 2397–2400.

Preis, K.; Bíró, O.; Reisinger, H.; Papp, K.; Ticar, I. 2008: "Eddy current losses in large air coils with layered stranded conductors", *IEEE Transactions on Magnetics*, Volume 44, Issue 6, June 2008, pp. 1318–1321.

Reichert, K.; Skoczylas, J.; Tarnhuvud, T. 1988: "Eddy current calculations in electrical machines; Numerical solution technique and accuracy problems", *Proceedings of International Conference on Electrical Machines*, Volume 2, 12–14 September 1988, Pisa, Italy, pp 59–64.

Richter, R. 1951: "Elektrische Maschinen" Verlag Birkhäuser Basel, Switzerland.

Saari, J. 1998: "Thermal analysis of high-speed induction machines", *Acta Polytechnica Scandinavica, Electrical Engineering series* No. 90. Espoo, Finland. (1998) 73 p. Available: http://lib.tkk.fi/Diss/199X/isbn9512255766/

Sabariego, R. V.; Dular, P.; Gyselinck, J. 2008: "Time-Domain Homogenization of Windings in 3-D Finite Element Models", *IEEE Transactions on Magnetics*, Volume 44, Issue 6, June 2008, pp. 1302–1305.

Sadowski, N.; Lefevre, Y.; Lajoie-Mazenc, M.; Cros, J. 1992: "Finite element torque calculation in electrical machines while considering the movement", *IEEE Transactions on Magnetics*, Volume 28, Issue 2, March 1992, pp. 1410–1413.

Salon, S. J.; Ovacik, L.; Balley, J. F. 1993: "Finite element calculation of harmonic losses in AC machine windings", *IEEE Transactions on Magnetics*, Volume 29, Issue 2, March 1993, pp. 1442–1445.

Seman, S.; Iov, F.; Niiranen, J.; Arkkio, A. 2006a: "Comparison of simulators for variable-speed wind turbine transient analysis", *International Journal of Energy Research,* Volume 30, Issue 9, April 2006, pp.713–728.

Seman, S.; Niiranen, J.; Arkkio, A. 2006b: "Ride-through analysis of doubly fed induction wind-power generator under unsymmetrical network disturbance", *IEEE Transactions on power Systems,* Volume 21, Issue 4, November 2006, pp. 1782–1789.

Seman, S.; Niiranen, J.; Kanerva, S.; Arkkio, A.; Saitz, S. 2006c: "Performance study of a doubly fed wind-power induction generator under network disturbances", *IEEE Transactions on Energy Conversion*, Volume: 21, Issue: 4, December 2006, pp. 883–890.

Seman, S. 2006: "Transient performance analysis of wind-power induction generators", TKK Dissertation 45, Espoo 2006, 112 p. Available: http://lib.tkk.fi/Diss/2006/isbn9512284235/

Silvester, P. 1966: “Modal network theory of skin effect in flat conductors”, *Proceedings of the IEEE*, Volume 54, Issue 9, September 1966, pp. 1147–1151.

Silvester, P. 1967: “AC resistance and reactance of isolated rectangular conductors”, *IEEE Transactions on Power Apparatus and Systems,* Volume 86, Issue 6, June 1967, pp.770–774.

Silvester, P. 1968: “The accurate calculation of skin effect in conductors of complicated shape”, *IEEE Transactions on Power Apparatus and Systems,* Volume 87, Issue 3, March 1968, pp. 735–74.

Silvester, P. 1969: “Skin effect in multiple and polyphase conductors” *IEEE Transactions on Power Apparatus and Systems,* Volume 88, Issue 3, March 1969, pp. 231–238.

Silvester, P.; Wong, S. K.; Burke, P. E. 1972: “Modal Theory of Skin Effect in Single and Multiple Turn Coils” *IEEE Transactions on Power Apparatus and Systems,* Volume 91, Issue 1, January 1972, pp. 29–34.

Stoll, R. L. 1974: “The analysis of eddy currents”, Clarendon Press, Oxford.

Sullivan, C. R. 2001: “Computationally efficient winding loss calculation with multiple windings, arbitrary waveforms, and two-dimensional or three-dimensional field geometry”, *IEEE Transactions on Power Electronics*, Volume 16, Issue 1, January 2001 pp. 142–150.

Szücs, Á.; Arkkio, A. 1999: “Consideration of eddy currents in the multi-conductor windings using the finite element method and the elimination of the inner nodes”, *IEEE Transactions on Magnetics*, Volume 35, Issue 3, May 1999, pp. 1147–1150.

Szücs, Á. 2000: “Macro elements in the finite element analysis of multi-conductor eddy current problems”, *IEEE Transactions on Magnetics*, Volume 36, Issue 4, July 2000, pp. 813–817.

Szücs, Á. 2001: “Macro element method for modeling eddy currents in the multi-conductor windings of electrical machines”, *Acta Polytechnica Scandinavica, Electrical Engineering series* No. 106. Helsinki, Finland. 88 p. Available: http://lib.tkk.fi/Diss/2001/isbn9512256916/

Tapia, A.; Tapia, G.; Ostolaza, J. X., Saénz, J. R. 2003: “Modeling and control of a wind turbine driven doubly fed induction generator”, *IEEE Transactions on Energy Conversion*, Volume 18, Issue 2, June 2003, pp. 194–204.

Takahashi, K.; Takahashi, M.; Sato, M. 2003: “Calculation method for strand current distributions in armature winding of a turbine generator”, *Electrical Engineering in Japan*, Volume 143, Issue 2, pp. 50–58.

Tsukerman, I. A.; Konrad, A.; Lavers, J.D. 1992: “A method for circuit connections in time-dependent eddy current problems”, *IEEE Transactions on Magnetics*, Volume 28, Issue 2, March 1992, pp. 1299–1302.

Tsukerman, I. A.; Konrad, A.; Meunier, G.; Sabonnadiere, J.C. 1993: “Coupled field-circuit problems: trends and accomplishments”, *IEEE Transactions on Magnetics*, Volume 29, Issue 2, March 1993, pp. 1701–1704.

Tsukerman, I. A.; Konrad, A.; Bedrosian, G.; Chari, M.V.K. 1993: “A survey of numerical methods for transient eddy current problems”, *IEEE Transactions on Magnetics*, Volume 29, Issue 2, March 1993, pp. 1711–1716.

Tsukerman, I. 1995: “A stability paradox for time-stepping schemes in coupled field problems”, *IEEE Transactions on Magnetics*, Volume 31, Issue 3, May 1995, pp. 1857–1860.

Vogt, K. 1983: “Elektrische maschinen”, 3rd Edition, Berlin, VEB Verlag Technik, 1983, 500 p.

Weiss, J.; Csendes, Z. J. 1982a: “A one-Step finite element method for multiconductor skin effect problems”, *IEEE Transactions on Power Apparatus and Systems,* Volume 101, Issue 10, October 1982, pp. 3796–3803.

Weiss, J.; Cendes, Z. 1982b: “Efficient finite element solution of multipath eddy current problems”, *IEEE Transactions on Magnetics*, Volume 18, Issue 6, November 1982, pp. 1710–1712.

Weiss, J.; Garg, V. K.; Sternheim, E. 1983: “Eddy current loss calculation in multiconductor systems”, *IEEE Transactions on Magnetics*, Volume 19, Issue 5, September 1983, pp. 2207–2209.

Weiss, J.; Garg, V. K. 1985: “One step finite element formulation of skin effect problems in multiconductor systems with rotational symmetry”, *IEEE Transactions on Magnetics*, Volume 21, Issue 6, November 1985, pp. 2313–2316.

Weiss, J.; Garg, V. K. 1988: “Steady state eddy current analysis in multiply-excited magnetic systems with arbitrary terminal conditions” *IEEE Transactions on Magnetics*, Volume 24, Issue 6, November 1988, pp. 2676–2678.

Weiss, J.; Garg, V. K. 1989: “Finite element of transient eddy current problems with the time dependent excitations”, *International conference of Magnetics, Digests of INTERMAG -89,* 28 – 31 March 1989, pp. HC6–HC6.

Xue, X. D.; Cheng, K. W. E. 2006: “An Energy-Saving Scheme of Variable Voltage Control for Three-Phase Induction Motor Drive Systems”, *IEEE Conference Record of the 2nd International Conference on Power Electronics Systems and Applications*, 12 – 14 November 2006, pp. 241–243.

Yamada, S.; Bessho, K.; Lu, J. 1989: “Harmonic balance finite element method applied to nonlinear AC magnetic analysis” *IEEE Transactions on Magnetics*, Volume 25, Issue 4, July 1989, pp. 2971–2973

Yamada, S.; Biringer, P. P.; Bessho, K. 1991: “Calculation of nonlinear eddy-current problems by the harmonic balance finite element method” *IEEE Transactions on Magnetics*, Volume 27, Issue 5, September 1991, pp. 4122–4125.

Yatchev, I.; Arkkio, A.; Niemenmaa, A. 1995: “Eddy-current losses in the stator winding of cage induction motors”, *Laboratory of Electromechanics, Helsinki University of Technology,* Report 47, Finland, 1995, 34 p.

ISBN 978-952-248-254-9
ISBN 978-952-248-255-6 (PDF)
ISSN 1795-2239
ISSN 1795-4584 (PDF)